Russian Chemical Reviews **75** (1) 31 – 55 (2006) © 2006 Russian Academy of Sciences and Turpion Ltd

DOI 10.1070/RC2006v075n01ABEH002482

Modelling of the dynamic state of disperse systems

N B Uriev, I V Kuchin

Contents

I.	Introduction	31
II.	Fundamentals of the flow theory of disperse systems	32
III.	Computer simulation of disperse systems	44
IV.	Conclusion	53

Abstract. The review covers main theories and models of shear flow of suspensions and results of computer simulation of the properties of disperse systems under dynamic conditions. Emphasis is given to the state of aggregated and non-aggregated suspensions. The microstructure of disperse systems is demonstrated to play a crucial role in their bulk rheological properties. The causes and conditions of the appearance of macroscopic inhomogeneity, *i.e.*, discontinuity in highly concentrated systems are analysed and the specific features of microrheology of low-concentrated fractal colloidal gels are reviewed. The review describes the possibilities of the use of surfactants and vibration treatment for controlling the rheological properties of dispersions. The advantages and disadvantages of computer simulation of disperse systems are discussed and examples of application of these methods to the description of the dynamic state of suspensions are given. The bibliography includes 147 references.

I. Introduction

Many natural phenomena and various chemical engineering processes involve disperse systems under non-equilibrium conditions. Hence, both theoretical and applied studies of these systems are of considerable interest. In the present review, different aspects of the behaviour of dispersions under dynamic conditions are considered in terms of physicochemical dynamics of disperse systems.[1–3] This new field supplements and extends the traditional approach to investigation of the properties of such systems predominantly under static conditions.

The physicochemical dynamics of disperse systems deals with dynamic processes taking place in ensembles of dispersed-phase particles held together by dispersion forces to form three-dimensional structural networks. Besides, it is concerned with the mechanisms of destruction of such systems under dynamic force conditions giving rise to particle aggregates (their evolution and interactions with each other and with a dispersion medium) and the reverse processes (structure formation under these conditions).[1] These problems are directly related to physicochemical hydrodynamics, including hydrodynamics of capillary systems.[4]

N B Uriev, I V Kuchin A N Frumkin Institute of Physical Chemistry and Electrochemistry, Russian Academy of Sciences, Leninsky prosp. 31, 119991 Moscow, Russian Federation. Fax (7-495) 955 46 79, tel. (7-495) 955 46 42, e-mail: uriev@phyche.ac.ru (N B Uriev), u912@yandex.ru (I V Kuchin)

Received 29 June 2005
Uspekhi Khimii **75** (1) 36 – 63 (2006); translated by T N Safonova

The ultimate aim of research in the area of physicochemical dynamics of disperse systems is to substantiate ways and procedures for achieving the maximum fluidity, which is necessary for intensification of various chemical engineering processes.[1] The control of the properties of suspensions, *viz.*, disperse systems, which are widely used in all fields of human activity, is of particular importance.

Theoretical analysis in physicochemical dynamics is based primarily on the construction of microrheological models that describe processes of interactions between particles, microstructure formation, microstructure transformations and degradation under external forces. These microprocesses determine the structural-rheological properties of suspensions characterising their response to mechanical forces.

Theoretical views of the features of microprocesses provide the basis for developing new procedures for controlling the properties of disperse systems under dynamic conditions and improving the available methods. Some rheological theories of suspensions and powders were analysed in the monograph.[5]

The continuing progress in computer technology offers opportunities to solve problems (in particular, to describe a microstructure of a medium), which are impossible to solve by analytical methods. Computer simulation occupies an intermediate place between theoretical and experimental studies. Computer experiments are based on theoretical models and are performed by numerical calculations. The models can become more complicated (to achieve better correspondence with experimental conditions) with progress in computer technology. Therefore, on the one hand, areas of theoretical research are expanded, and, on the other hand, it becomes possible to perform numerous repeated expensive experiments. Consequently, computer simulation is an important bridge between the theory and experiment.[6]

The efficiency of application of computer simulation to the dynamics of disperse systems is determined by several factors. First, theoretical models are often based on phenomenological equations, which describe phenomena at the macrolevel and ignore many microscopic features of the system. As a rule, this problem can be solved by numerical methods (in particular, a detailed view of the dynamics of structuring and microstructure transformations can be obtained). Second, computer simulation can be used as a rather efficient procedure for validating analytical theories of structures and properties of disperse systems. Third, computer simulation allows one to examine the behaviour of systems under conditions that are difficult to observe in practice (high flow rates, vibration treatment, *etc.*). In addition, this method provides information on parameters that are impossible to measure (the number of coagulation contacts between particles and the rate at which they are broken, shear stresses separately in

the liquid and solid phases, *etc.*). In some cases, the difficulties can be associated with hazardous experimental conditions and high cost of experiments. Because of this, computer simulation is a convenient and efficient tool for investigating the structures and properties of disperse systems. However, data obtained by this method should be compared with theoretical and experimental estimates because the results of numerical calculations may contain uncertainty due to specific features of the system under study and limitations of a particular simulation method.

The present review covers analytical and computer models used for describing the behaviour of an important class of disperse systems, *viz.*, suspensions, under dynamic conditions and predicting their structural-rheological properties.

II. Fundamentals of the flow theory of disperse systems

1. Non-structured disperse systems

The dependence of the effective suspension viscosity on the concentration of the solid phase is most simply described by the Einstein equation

$$\eta = \eta_0\left(1+\frac{5}{2}\varphi\right), \tag{1}$$

where η_0 is the viscosity of a pure liquid (dispersion medium) and φ is the concentration of the solid phase.

This equation is valid for highly dilute non-structured suspensions where interactions between particles can be ignored. The equation reflects an increase in the suspension viscosity due to hydrodynamic effects caused by solid particles introduced into the flow and takes into account the energy dissipation for rotation of particles in a shear flow.

If the concentration of solid particles increases so that interactions between the particles become significant, Eqn (1) provides poor agreement with experimental data. Hydrodynamic interactions can be taken into account, to some extent, by introducing higher-order terms with respect to φ (φ^2, φ^3, *etc.*). If only pair interactions are considered,[7] the dependence of the suspension viscosity on the concentration of the solid phase can be described by the equation:

$$\eta = \eta_0\left(1+\frac{5}{2}\varphi + a\varphi^2\right). \tag{2}$$

The coefficient a is a function of the concentration φ and the particle sizes and coordinates. This coefficient is calculated by complex statistical methods. The following dependence $a(\varphi)$ was obtained [9] with the use of the Percus – Yevick equation:[8]

φ	0.0	0.1	0.2	0.3	0.4	0.5	0.6
a	5.00	5.38	5.81	6.31	6.91	7.65	8.66

The results of calculations according to Eqn (2) taking into consideration the dependence $a(\varphi)$ are in satisfactory agreement with experimental data at $\varphi \leqslant 0.25$. At higher concentrations, calculations by Eqn (2) underestimate the viscosity η, which indicates that it is necessary to take into account perturbations of the velocity fields about the particle caused by the influence of adjacent particles. Evidently, these calculations present considerable mathematical difficulties. However, there is a number of models and approximate methods that enable one to find the dependence $\eta(\varphi)$ up to the highest concentrations.

Of semiphenomenological equations describing the dependence of the suspension viscosity of spherical particles on their concentration throughout the range of φ, the Mooney equation [10]

$$\frac{\eta}{\eta_0} = \exp\left(\frac{\alpha\varphi}{1-\varphi/\varphi_\mathrm{m}}\right) \tag{3}$$

and the Krieger – Dougherty equation [11, 12]

$$\frac{\eta}{\eta_0} = \left(1-\frac{\varphi}{\varphi_\mathrm{m}}\right)^{-\alpha\varphi_\mathrm{m}} \tag{4}$$

have gained wide acceptance. Here φ_m can be identified with the volume fraction of closely-packed particles (random packings of particles with φ_m varying from 0.59 to 0.65 are most typical of suspensions). The coefficient α is chosen such as to provide the agreement of Eqns (3) and (4) with the Einstein equation ($\alpha = 2.5$).

The results of calculations according to Eqn (4) are in somewhat better agreement with experimental data as compared to the Mooney equation. As mentioned above, the common drawback of these equations is their semiphenomenological character. The derivation of these equations was not based on theoretically supported microrheological views of the character of flow of concentrated disperse systems. In this respect, a more correct approach is based on the use of various cellular models that have been proposed for the first time in the publications.[13–15] Within these models, it is generally assumed that the cell consists of a rigid spherical shell whose centre is occupied by the spherical particle under consideration. The velocity of the liquid within a circular layer between the particle and the sphere is estimated by the Stokes equation [16] taking into account certain boundary conditions. With a knowledge of the velocities and mechanical stresses at the cell boundary, it is possible to calculate the energy dissipated in the cell containing a particle (E_1) and without this particle (E_0). The suspension viscosity is determined from the equation [14]

$$\frac{\eta}{\eta_0} = \frac{E_1}{E_0}. \tag{5}$$

One of the most perfect cellular models, which is sometimes called the free surface model, was proposed by Happel.[14, 15] Within this model, the viscosity is calculated according to the equation

$$\frac{\eta}{\eta_0} = 1 + 5.5\varphi\,\frac{4\varphi^{7/3} + 10 - (84/11)\varphi^{2/3}}{10(1-\varphi^{10/3}) - 25\varphi(1-\varphi^{4/3})}. \tag{6}$$

A substantial drawback of cellular models is that the cell shape is chosen arbitrarily. A spherical cell is simple for analysis. However, the results obtained with the use of this model at high concentrations of the solid phase are in poor agreement with experimental data. This is associated with the fact that with $\varphi \to \varphi_\mathrm{m}$ the distance between the particles decreases to an extent that it becomes necessary to consider the liquid flow in microchannels between the particle surfaces.

This model has been considered for the first time by Frankel and Acrivos.[17] This model is sometimes called the lubrication model because it is based on the lubrication theory. The model treats a test particle surrounded by z adjacent particles equidistant from the test particle. The cell consists of a sphere with a radius $r + h/2$ (r is the radius of the test particle and h is the distance between the particle surfaces). The test particle lies in the centre of the cell coinciding with the origin of coordinates. At $z = 6$ (which corresponds to a random close packing [18]), the centres of the adjacent particles lie on the Cartesian axes (x, y, z) (Fig. 1). It is hypothesised that an elongational flow occurs in suspensions. The hydrodynamic resistance to motion of each adjacent particle relative to the central particle is calculated according to the equations of the lubrication theory.[7] It is assumed that the energy dissipation velocity is determined by both the perturbation of the velocity field with a single sphere and the sum of flows in microchannels between particle pairs. This model gives quantitative results for $\varphi \to \varphi_\mathrm{m}$ when $h/2r \to 0$. The following equation for the suspension viscosity was derived from Eqn (5):[17]

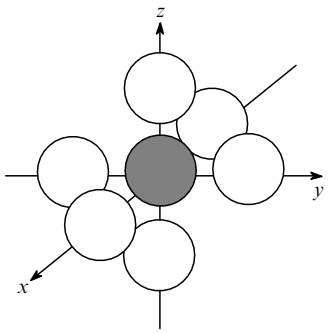


Figure 1. Arrangement of particles in the lubrication model. The shaded particle is surrounded by 6 particles.

$$\frac{\eta}{\eta_0} = \frac{3z}{16}\frac{1}{(\varphi_m/\varphi)^{1/3} - 1}. \quad (7)$$

Frankel – Acrivos's model was criticised many times. In particular, it was noted [19] that it is incorrect to extend the results, which were obtained for an elongational flow under the assumption of a special arrangement of particles, to a shear flow. It was demonstrated [20] that the application of the lubrication theory to the particle motion performed by parallel layers in a shear flow gives only the logarithmic dependence of the suspension viscosity on $2r/h$ when $h \to 0$, whereas experiments showed that η more sharply increases with $\varphi \to \varphi_m$. The inclusion of other factors influencing the viscosity (for example, rotation of adjacent particles) does not change the logarithmic character of the dependence $\eta(\varphi)$. This led to the conclusion [5] that particles of a suspension in a shear flow move chaotically rather than are arranged in layers. In this case, the lubrication model becomes more correct, because particles inevitably approach each other during chaotic motion, the liquid serving as a lubricant between the particle surfaces. Assuming that particles move chaotically, the equation analogous to Eqn (7) was derived [21] with the use of the dense gas kinetic theory.

Another way of describing the configuration of particles surrounding the test particle is based on an effective medium model.[22] Within this model, the configuration of particles is considered as a particular effective homogeneous medium containing the test particle. The viscosity of the medium η^* is equal to the viscosity of a pure liquid η_0 on the surface of the test particle, increases with increasing distance from this surface and is identified with the viscosity of the suspension as a whole at infinity

$$\eta^* = \eta_0 + (\eta - \eta_0)\psi(x, \varphi), \quad (8)$$

where $\psi(x,\varphi)$ is a function of the particle coordinates and concentration.

The field of velocity perturbations (u) induced by the test particle in the medium is determined by the Stokes equations,[16] which are written for this model taking into account the dependence $\eta^*(x)$

$$\nabla p = \nabla(\eta^* \nabla \boldsymbol{u}), \nabla \boldsymbol{u} = 0$$

The simplest assumption about the change in η^* can be made by identifying the effective medium with a suspension as a whole, *i.e.*, taking $\psi = 1$. This assumption,[23] which corresponds to the mean-field model widely accepted in physics, gives the following equation for the average stress tensor:

$$\langle \hat{\sigma} \rangle = 2\hat{E}\eta_0 + 5\varphi\eta\hat{E}, \quad (9)$$

where $\hat{E}$ is the strain rate tensor.

From Eqn (9), the following equation for the relative suspension viscosity was derived:[23–25]

$$\frac{\eta}{\eta_0} = \frac{1}{1 - (5/2)\varphi}. \quad (10)$$

At small φ, this equation turns into Eqn (2). At high concentrations, the viscosities calculated according to Eqn (10) are overestimated. Evidently, this is associated with an arbitrary choice of the function $\psi(x,\varphi)$. To obtain more accurate results, a more realistic function ψ should be used in the effective medium model. However, in this case, it is impossible to derive analytical equations for the suspension viscosity due to mathematical difficulties.

The results of calculations according to Eqns (4), (6), (7) and (10) and experimental dependences of the viscosity of poly(methyl methacrylate) (PMMA) in decalin are presented in Fig. 2. A comparison of the curves shows that the results obtained with the use of the effective medium model and the free surface model agree with experimental data at low concentrations ($\varphi < 0.4$), whereas the results obtained with the use of the lubrication model are in agreement with experimental data at high concentrations ($\varphi > 0.4$). In the calculations, φ_m was taken to be 0.61, which corresponds to conditions of many experiments. Detailed analysis of the possibilities of using the above-considered models for the description of the viscosity of non-aggregated and aggregated suspensions was performed in the study.[26]

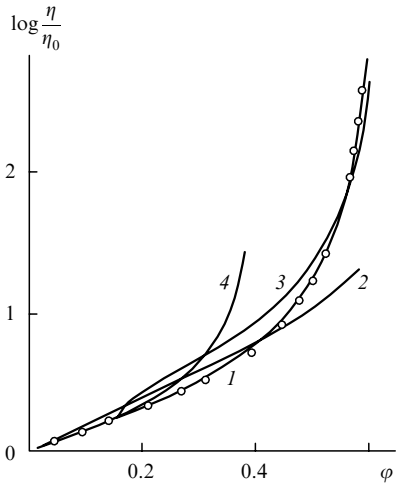


Figure 2. The relative suspension viscosity *vs.* the volume fraction of particles.[26]
Curves (*1–4*) were calculated according to Eqns (4), (6), (7 at $z = 6$) and (10), respectively; the points correspond to the experimental data [27] for PMMA particles ($d = 0.5$ μm) in decalin (the viscosity for $\dot{\varepsilon} \to \infty$).

The influence of Brownian motion of particles on the viscosity of suspensions formed by these particles can be taken into consideration with the use of the Peclet number

$$\mathrm{Pe} = \frac{d^2\dot{\varepsilon}}{D},$$

where d is the particle size, $\dot{\varepsilon}$ is the shear rate and D is the particle diffusion coefficient.

The suspension viscosity can be represented as a function of the only parameter, *viz.*, the Peclet number [28]

$$\frac{\eta - \eta_\infty}{\eta_1 - \eta_\infty} = \frac{1}{1 + \mathrm{Pe}/\mathrm{Pe_c}}, \quad (11)$$

where η_1 and η_∞ are the suspension viscosities at $\mathrm{Pe} \ll \mathrm{Pe_c}$ and $\mathrm{Pe} \gg \mathrm{Pe_c}$, respectively, and $\mathrm{Pe_c} \approx 1$ is the critical value of the Peclet number.

Brownian suspensions of spherical particles were studied experimentally in broad ranges of particle concentrations and sizes.[29–31] The results of these studies agree well with the results of calculations according to Eqn (11), $\mathrm{Pe_c}$ being dependent on φ. It

was found that $Pe_c = 1.5$ at $\varphi = 0.2$ and $Pe_c \to 0$ at $\varphi \to \varphi_m = 0.6$, *i.e.*, the influence of the Brownian motion on the suspension viscosity decreases as the packing of particles approaches the close-packing density. At the same time, as was demonstrated in the studies,[9,32] the Brownian motion in dilute suspensions, for which the function $\eta(\varphi)$ can be expanded in a power series of φ, has an effect only on the quadratic term accounting for particle-pair interactions. The linear term in Eqn (2) is independent of the Peclet number.

Therefore, the Brownian motion influences most substantially the rheological properties of suspensions at a concentration $\varphi \approx 0.1-0.2$. However, this conclusion is true only for suspensions composed of strictly spherical particles. If the Brownian motion is taken into account in the case of anisometric particles, it is the linear term in Eqn (2) that becomes dependent on the Peclet number due to reorientation of the particles in a flow.

The development of a unified two-phase model for suspensions and powders [5,21] has assisted in developing the rheological theory of disperse systems. The use of this model made it possible to derive the general equation, which is valid at low and high viscosities of a medium for powders and suspensions, respectively. This model was based on the lubrication model,[17] which treats the test particle moving among z surrounding stationary particles. The following equation for the viscosity of a system of rigid spheres in a viscous medium was derived with the use of the Eyring equation of state:[33]

$$\eta \approx 0.16\varphi_m \alpha \frac{\rho d \upsilon}{\left[(\varphi_m/\varphi)^{1/3} - 1\right]\left[1 - \exp(-\upsilon/\upsilon_c)\right]}, \qquad (12)$$

where α is the coefficient that depends on the parameters of particle collisions, ρ is the particle density, υ is the velocity at which particles approach each other and $\upsilon_c = (9/4)z\eta_0/\rho d$ is the value identified with the minimum velocity υ, which must be imparted to particles in order that they overcome the hydrodynamic resistance on collisions.

For two limiting flow types, the following equations were derived for the viscosity of a system when $\varphi \to \varphi_m$:[5]

$$\eta \approx \frac{c_1\eta_0}{(\varphi_m/\varphi)^{1/3} - 1} \text{ at } \upsilon \ll \upsilon_c, \qquad (13)$$

$$\eta \approx \frac{c_2\rho d\upsilon}{(\varphi_m/\varphi)^{1/3} - 1} \text{ at } \upsilon \gg \upsilon_c. \qquad (14)$$

Here $c_1 \approx 0.1$ and $c_2 \approx 0.05$.

For particle collisions, the hydrodynamic factor plays the determining role in the former case [Eqn (13)], *i.e.*, the viscosity of the system is determined by the energy dissipation in a flow in the space between the particles. This is typical of suspensions. Equation (14) is valid for low-viscosity media, where the viscosity is determined by the energy dissipation due to inelasticity of particle collisions, which is characteristic of powders. The advantage of Eqn (12) is that it is universal and describes both limiting flow types. Equation (13) corresponding to suspensions is equivalent to Eqn (7), which was derived in another way, by comparing the energy dissipated in a unit volume of a suspension with the energy supplied to the system upon its shear deformation. The drawbacks of Eqns (12)–(14) are that they are based on two-particle collisions, which, in the case of concentrated systems, is unlikely to be justified.

2. Structured disperse systems

The above-considered rheological models describe the viscosity of non-structured systems. However, it is known that the structure formation in disperse systems leads to a drastic change in their rheological properties.[34] The rheological properties of structured disperse systems under conditions of their continuous shear deformation are most often described with the use of the overall rheological flow curve, *e.g.*, the plot of the effective shear viscosity *vs.* the shear rate $\dot{\varepsilon}$ (or the shear stress σ) on condition that destruction is isotropic. The overall flow curve with a viscosity drop of up to 8–10 orders of magnitude was described for the first time in the study.[35] In this study, the authors introduced the concepts of 'the highest viscosity of a virtually non-destroyed structure' corresponding to the upper plateau in the flow curve and 'the lowest Newtonian' viscosity of a maximum destroyed structure. More recently, it has been demonstrated [1–3] that the true maximum destruction can be achieved only under shear deformation used along with other external mechanical forces (for example, vibration), as well as by lyophilisation of the particle surface with surfactants.

To estimate the fluidity of structured systems, certain assumptions about the character of structuring should be made. There are two types of such assumptions and the corresponding structural models of disperse systems. Models of one type treat particles that are held together to form a continuous structure. Its homogeneity is retained, under deformation, at distances much larger than the particle diameter. Parameters having the dimensionality of length are not used for the description of the structure. In another type of models, the structures are composed of particle aggregates. The parameter characterising inhomogeneity of the structure is generally identified with the aggregate size.[5]

Thus, simulation is the main method of theoretical studies of structured systems. This is associated with the lack of experimental methods that would allow one to study in-depth the structures of disperse systems and their changes in flow. The available methods have been insufficiently developed. Only rheological experiments provide reliable data on the structures, the construction of alternative microrheological models being a necessary step in these investigations.

In the study,[21] the rheological properties of a system were related to its structural characteristics, such as the diameter of spherical aggregates and the distance between their centres. It was assumed that deaggregation in flow occurs due to detachment of particles from the aggregate surface until an equilibrium state is established at a given shear rate $\dot{\varepsilon}$, at which further detachment of particles becomes impossible. The space between the aggregates is filled with a suspension of particles detached from the aggregate surface. The viscosity of this suspension is equal to that of completely deaggregated system of spheres at the same concentration, *i.e.*, to the viscosity of this system after its complete destruction.

Under the assumptions used for deriving Eqns (13) and (14), the following equation was obtained [21] for the dependence of the viscosity of a weakly aggregated suspension on the shear rate:

$$\frac{\eta}{\eta_\infty} = \left(\frac{\dot{\varepsilon}_c}{\dot{\varepsilon}}\right)^{1/2}, \qquad (15)$$

where η_∞ is the viscosity when $\dot{\varepsilon} \to \infty$, $\dot{\varepsilon}_c = 6.4F/(\eta_\infty d^2) = 6.4k'/(\eta_\infty d)$ is the critical shear rate $\dot{\varepsilon}$ corresponding to the complete deaggregation, F is the strength of bonding between the particles and k' is the coefficient that depends on the nature of the surface forces.

Equation (15) can be used at shear rates $\dot{\varepsilon}_c(L_1/L_2)^2 \ll \dot{\varepsilon} \ll \dot{\varepsilon}_c$, where L_1 is the average distance between the particles and L_2 is the average distance between the centres of aggregates. At $\dot{\varepsilon} < \dot{\varepsilon}_c(L_1/L_2)^2$, the distance between the aggregate surfaces is comparable to the particle diameter and this equation is inapplicable. Equation (15) does not include the aggregate diameter and contains only parameters having a precise physical meaning, such as the viscosity of the completely destructured system η_∞, which can be interpreted as the minimum viscosity at high $\dot{\varepsilon}$ until dilatancy appears, and the coefficient k'. The latter is expressed in terms of the Hamaker constant A (see Refs 36 and 37) and the distance between the particle surfaces. Hence, with a knowledge of A, it is possible to determine the shape of the rheological curve. If the constant A is unknown, the order of A in this system can be estimated by measuring η_∞ and $\dot{\varepsilon}_c$.

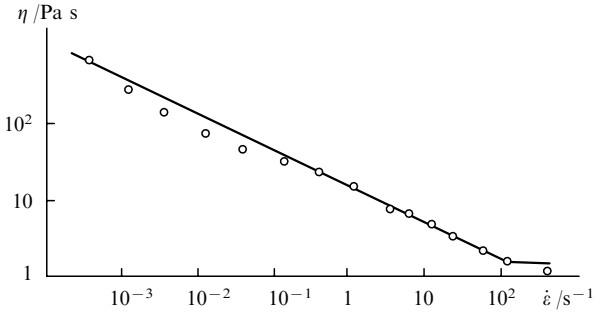


Figure 3. Calculated curve and experimental data (points) for a PMMA suspension in decalin ($\varphi = 60.1\%$, $d = 0.47$ μm, $\eta_0 = 2.8$ mPa s at $T = 293$ K).[21]

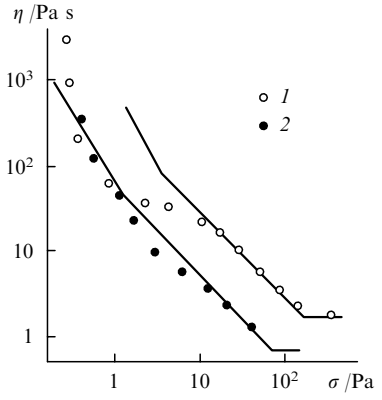


Figure 4. Effective viscosity η *vs.* the shear stress for a PMMA suspension in decalin at $\varphi = 60.1$ (*1*) and 59.5% (*2*).[38]

In spite of a good agreement between the experimental data and the results of calculations according to Eqn (15) for a monodisperse suspension of PMMA particles in decalin (Fig. 3), this equation is of limited application. Actually, the dependence of the suspension viscosity on the shear rate

$$\eta \sim \dot{\varepsilon}^{-1/2}$$

describes well the region of intermediate gradients for a model system considered in the study.[21] However, for many other systems, even if this dependence at intermediate gradients is searched in the form

$$\eta \sim \dot{\varepsilon}^{-n},$$

n can vary from 1/2 to 1.[38] In addition, at small $\dot{\varepsilon}$ the dependence $\eta(\dot{\varepsilon})$ generally becomes sharper, including that for the model system described in the study.[21] The way of generalising Eqn (15), according to which n can assume the values $> 1/2$, and the relationship between n and the structural characteristics were discussed.[38] The authors believed that aggregates can form higher-order structures, *viz.*, superaggregates. The motion of superaggregates is treated in a non-aggregated suspension serving as a non-Newtonian medium, and the viscosity is determined according to Eqn (15). Under these assumptions, the following equation was obtained for the viscosity of strongly aggregated suspensions:

$$\frac{\eta}{\eta_\infty} = B\left(\frac{3k+1}{2k}, \frac{3-k}{2k}\right)\frac{3 \times 2^{1/k}(2+k)^{1/k}}{4} \times \left[\frac{p\dot{\varepsilon}_c^{2(k+1)/(3-k)}}{(2+k)^{1/k}2^{1/k}\eta_\infty \dot{\varepsilon}^{(k+1)/(3-k)}} \times \frac{1}{B((k+1)/2k, (3+k)/2k)}\right]^{(3-k)/(3+k)}. \quad (16)$$

Here $B(\ldots, \ldots)$ is the β function, $k = 1/(1-n)$ and p is the strength of the superaggregates.

In particular, at $n = 0$ and $k = 1$, Eqn (16) can be represented as Eqn (15).

At concentrations $\varphi < 60\%$, the rheological curves, which were constructed with the use of the notions of the aggregation mechanism, agree well with experimental data throughout the range in which the shear stress σ was varied (Fig. 4). However, at $\varphi > 60\%$ and low σ, a substantial deviation from this dependence was observed, and the curve has a plateau, which can be attributed to discontinuity of structure. This phenomenon, its possible manifestations and factors responsible for its occurrence both in well-characterised disperse systems and systems formed by polydispersed (in some cases, anisometric) particles of dispersed phases in liquid media were analysed in-depth.[39,40] The conditions determining the possibility of discontinuities under deformation of concentrated disperse systems were formulated in the study.[41]

In real systems with a non-uniform packing of particles in a quasi-crystal lattice, accumulations of vacancies, *i.e.*, cavities free from dispersed particles, are present. As in the crystalline substances, these cavities can be transformed into discontinuities (cracks) under shear stresses. The possibility of an increase in the cavity size is determined by the ratio of the relaxation times of the following processes that occur in the vicinity of this cavity under deformation of the system:[41]

elastic energy release due to the development of discontinuity

$$\tau_1 \sim l\frac{(\rho G)^{1/2}}{\sigma};$$

the formation of a new surface due to the development of a macroscopic crack

$$\tau_2 \sim l\left(\rho\frac{l}{\gamma}\right)^{1/2};$$

the mass transfer to the discontinuity zone as a result of vacancy drift

$$\tau_3 \sim \frac{l}{a}\sqrt{\frac{m\Delta^2}{U_0}}\exp\left(\frac{U_0}{k_B T}\right) \times \left[\sqrt{1+\frac{m\Delta^2}{U_0}\left(\frac{\eta_0}{\rho a h}\right)^2} - \sqrt{\frac{m\Delta^2}{U_0}}\frac{\eta_0}{\rho a h}\right]^{-1} \times \left[\exp\left(\frac{\sigma a^2 \Delta}{k_B T}\right) - \exp\left(-\frac{\sigma a^3}{k_B T}\right)\right]^{-1}.$$

Here l is the linear size of the cavity in the quasi-crystal lattice, $G \sim F/\Delta a$ is the shear modulus, ρ is the density of the solid phase, $\gamma \sim U_0/a^2 \sim F\Delta/a^2$ is the specific surface energy, a is the quasi-crystal lattice spacing, Δ and U_0 are the half-height and half-width of the potential well, respectively, h is the distance between the particle surfaces and m is the particle mass.

The equations for the relaxation times of the first two processes were derived based on the dimensionalities of the physical parameters. The latter equation was obtained based on the Frenkel and Eyring hole theories assuming that the motion of dispersed particles is analogous to that of molecules of the liquid.

The development of discontinuity occurs if the relaxation time of elastic energy release (τ_1) is shorter than the relaxation times of processes, which can hinder the appearance of discontinuities (τ_2 and τ_3), *i.e.*, on the condition [41]

$$\frac{1}{\tau_1} \gg \frac{1}{\tau_2} + \frac{1}{\tau_3} \tag{17}$$

or

$$\sigma \gg \frac{F_c}{a^2}\sqrt{\frac{a}{l}} + G\left[\exp\left(\frac{\sigma a^2 \Delta}{k_B T}\right) - \exp\left(-\frac{\sigma a^3}{k_B T}\right)\right] \times$$

$$\times \exp\left(-\frac{U_0}{k_B T}\right) \times \left[\sqrt{1 + \frac{m\Delta^2}{U_0}\left(\frac{\eta_0}{\rho a h}\right)^2} - \sqrt{\frac{m\Delta^2}{U_0}}\,\frac{\eta_0}{\rho a h}\right].$$

This condition is fulfilled at

$$\sigma_1 \ll \sigma \ll \sigma_2\,, \tag{18}$$

where σ_1 and σ_2 are determined from the equations

$$\sigma_1 \sim p_h\left(\frac{a}{l}\right)^{1/2}, \tag{19}$$

$$\sigma_2 \sim p_h - \frac{k_B T}{a^2 \Delta} \times \tag{20}$$

$$\times \ln\left\{\frac{G}{\sigma_2}\left[\sqrt{1 + \frac{m\Delta^2}{U_0}\left(\frac{\eta_0}{\rho a h}\right)^2} - \sqrt{\frac{m\Delta^2}{U_0}}\,\frac{\eta_0}{\rho a h}\right]\right\},$$

where $p_h \sim F/a^2$ is the shear strength of an ideal (homogeneous) structure.

The development of discontinuity as a result of deformation occurs only at σ corresponding to the range (18), if the packing of particles was inhomogeneous before deformation. Under lower or higher shear stresses, a homogeneous viscous flow occurs. The structure inhomogeneity (regions with a closer packing) serve as nucleation sites for discontinuities. The parameters σ_1 and σ_2 calculated according to Eqns (19) and (20), respectively,[41] are in satisfactory agreement with experimental data.

Some models of structured systems are based on the Eyring viscosity theory. This theory was used for deriving the equation for the viscosity of flocculated colloidal dispersions [42]

$$\eta = (\eta_1 - \eta_\infty)\frac{[\mathrm{sh}(\beta\dot{\varepsilon})]^{-1}}{\beta\dot{\varepsilon}} + \eta_\infty\,, \tag{21}$$

where η_1 and η_∞ are the limiting viscosities of the suspension when $\dot{\varepsilon} \to 0$ and $\dot{\varepsilon} \to \infty$, respectively;

$$\beta = k\frac{d^2}{D}\left(\frac{U}{k_B T}\right)^{-1}\exp\left(\frac{U}{k_B T}\right),$$

k is the proportionality coefficient that depends on the properties of the structure and U is the activation energy (potential barrier to particle shear migration).

The activation energies U were calculated by Churaev on the assumption that particles are fixed in the sites of a body-centred cubic lattice.[43] The migration of the particle A to the vacant site B through the potential barrier due to its interaction with the adjacent particles was considered. The potential barrier was calculated by summarising the energies of pair interactions between the particle A and the nearest neighbours. As a result, the forces acting on the transferred particle were determined taking into consideration the viscous resistance of interlaeyrs of the liquid between particles. The time dependence of the deformation rate determined from the migration rates of the particle A is similar to that found within the limits of the well-known Calvin rheological model with a variable viscosity. Using these calculation methods, an attempt was made to establish the functional relationship between the potential curves of particle pair interactions in a disperse system, on the one hand, and its structural-mechanical properties, on the other hand. It became possible to reveal changes in the structural-rheological parameters of a dispersion caused by changes in the electrolyte concentration, the surface charge, hydrophilicity of the particle surfaces and adsorption of surfactants and polymers on the particle surface. The drawback of the approach proposed [43] is that the properties of dispersions can be predicted only qualitatively.

In a model developed by Ogawa *et al.*,[44] the shear stress σ in colloidal suspensions can be divided into two components: the viscous stress and strain associated with interactions between particles. The first term can be determined from the Krieger–Dougherty equation (4). The second term depends on the interparticle potential and was determined based on a knowledge about activation processes. Hence, the equation for the relative viscosity can be written as follows

$$\frac{\eta}{\eta_0} = \left(1 - \frac{\varphi}{\varphi_m}\right)^{-2.5\varphi_m} + c_1\varphi\exp\left(\frac{U}{k_B T} - \frac{c_2 d^3\sigma}{\varphi k_B T}\right), \tag{22}$$

where c_1 and c_2 are numerical constants (theoretically equal to $\pi/6$). The height of the energy barrier U is taken to be proportional to the particle pair potential at the midpoint between the particles. The parameter φ_m is chosen so as to achieve an agreement with experimental data at $\eta_\infty = \eta(\sigma \to \infty)$ for a suspension of solid spheres.[29,45] With $\sigma \to 0$, Eqn (22) is identical to the equation corresponding to the model proposed earlier.[46] However, the author [46] considered U as the difference between the total potentials for the particles in the initial and final positions. The potentials were calculated taking into consideration the nearest neighbours under the assumption of a face-centred cubic lattice.

In the case of strong repulsions between the particles, the yield stress is described by the equation [44]

$$\sigma_y = \frac{\varphi U}{c_1 d^3}\,. \tag{23}$$

This equation is equivalent to the equation for σ_y reported in the study.[47] Equation (23) can be easily obtained with the use of an effective medium model and assuming that $c_1 = 1/3$ rather than $\pi/6$. For systems characterised by a considerable attraction between the particles, several equations relating the yield stress to the energy required for deaggregation were proposed. These models were reviewed in detail in the publication.[48]

In the study,[49] another class of models describing the viscosity of structured suspensions was considered. These models are based on approach including the following sequence of operations:

— a variable S that characterises the structure is introduced;

— the equation for the change in S under forces, which cause microstructure degradation (viscous friction forces in a shear flow) and assist in restoring the initial state (Brownian and dispersion forces) is written;

— the relationship between the viscosity and S is derived.

Let us consider one of the possible definition of the structural variable and its relationship with the suspension viscosity.[50,51] Dispersions are represented as mixtures of individual particles and groups of particles (structural units, aggregates) suspended in a liquid. Particles comprising a structural unit move together as a rigid cluster thus transferring the liquid immobilised in this cluster. Therefore, a decrease in the viscosity with increasing shear rate is considered as a result of rapid degradation of structural units, which is accompanied by an increase in both the concentration of individual particles and the free liquid volume. An increase in the viscosity is, on the contrary, related to the formation of new structural units in a shear flow. The characteristics of the structural units (the size, shape and the possibility of the appearance or destruction in a shear flow) depend substantially on the type of interactions between the particles. If attractive forces between the particles prevail, the structural units can exist as flakes, aggregates or clusters of aggregates. In some systems, small aggregates are held together so tightly that deaggregation does not occur under shear forces. Hence, such aggregates can be considered as individual particles.[52] If interactions are weak, the

structural units are merely groups of particles in a suspension of more or less free individual particles.

Let us denote the volume fractions of the structural units and individual particles by φ_s and $\varphi_p = \varphi - \varphi_s$, respectively. The structural variable can be given[50] as $S = \varphi_s/\varphi$. The effective volume fraction of the dispersed phase is

$$\varphi_{ef} = \frac{\varphi_s}{\varphi} + \varphi_p = \varphi(1 + CS),$$

where $C = 1/\varphi - 1$ is the compactness factor.

The equation specifying the change in S with time can be written as follows:

$$\frac{dS}{dt} = \frac{1}{\tau_1}(S_1 - S) - \frac{1}{\tau_2}(S - S_\infty), \tag{24}$$

where τ_1 and τ_2 are the characteristic relaxation times of the Brownian and hydrodynamic forces, respectively, and S_1 and S_∞ are the limiting values of the variable S when $\sigma \to 0$ and $\sigma \to \infty$, respectively. Under conditions of dynamic equilibrium, the variable S reaches a particular stationary value. In this case,

$$\frac{S_1 - S}{S - S_\infty} = \frac{\tau_1}{\tau_2} = \theta,$$

where θ is the kinetic ratio. For dilute suspensions of solid spheres, the time $\tau_1 \sim d^2/D$, which corresponds to the diffusion time of a particle to a distance comparable to its size. The characteristic time of hydrodynamic interactions in a shear flow τ_2 is similar in order of magnitude to $\dot{\varepsilon}^{-1}$. Consequently, θ in dilute systems is equal to the Peclet number $\mathrm{Pe} = d^2\dot{\varepsilon}/D$, which can be considered as the ratio of the viscous friction work to the energy of thermal motion of the particles. In concentrated suspensions, the diffusion motion of the particles is strongly hindered and the suspension viscosity is substituted into the equations for the characteristic times instead of the viscosity of a medium. Then

$$\theta \sim \frac{\sigma d^3}{k_B T}.$$

Assuming that $\theta = \sigma/\sigma_c$, the critical shear stress can be determined as

$$\sigma_c = \frac{k_B T}{d^3}.$$

This relationship is the known Krieger correction (for Brownian motion) for colloidal suspensions.[12]

In the last step, the relationship between the viscosity and the shear stress is determined. In the study,[50] the following equation, which describes the non-Newtonian behaviour of suspensions under conditions of shear stress, is derived:

$$\eta(\sigma) = \eta_\infty \left(\frac{1 + \sigma/\sigma_c}{R_r + \sigma/\sigma_c}\right)^2. \tag{25}$$

Here, the rheological index R_r is expressed by the equation

$$R_r = \frac{1 - \varphi/\varphi_1}{1 - \varphi/\varphi_\infty} = \begin{cases} (\eta_\infty/\eta_1)^{1/2} & \text{if } \varphi < \varphi_1 \\ -\sigma_y/\sigma_c & \text{if } \varphi \geqslant \varphi_1 \end{cases}, \tag{26}$$

where

$$\varphi_1 = \frac{\varphi_m}{1 + CS_1},$$

$$\varphi_\infty = \frac{\varphi_m}{1 + CS_\infty}.$$

At $\varphi < \varphi_1$, the calculated function $\eta(\sigma)$ represents a curve consisting of two regions, which correspond to the Newtonian viscosity at low and high shear stresses, and an intermediate region in which the viscosity decreases. The plateau corresponding to low shear stresses disappears as the concentration φ increases and approaches φ_1, *i.e.*, the yield point σ_y is achieved. At $\varphi > \varphi_1$, the system exhibits the plastic properties.[53] In addition, at $R_r > 1$ the model can reflect the dilatant properties of suspensions.[54, 55]

Let us consider the differential method used for calculating the effective properties of disperse systems. The method consists of the following. A dispersed phase is added portionwise to the system under study. In each step, the effective properties of the disperse system are calculated with the use of the effective properties of the system determined in the previous step. In the zeroth step, the disperse system does not contain a dispersed phase and consists completely of a dispersion medium. The effective coefficients are determined in each step using a linear approximation, which was obtained from solving the problem at a low concentration of the dispersed phase. This approach allows one to derive differential equations or related differential equation systems, which describe the dependence of the desired characteristics on the concentration of the dispersed phase. The effective constants of the disperse system can be determined by solving the differential equation system. In the studies,[56, 57] this method was used to calculate the effective characteristics of porous media, in particular, to evaluate the viscosity of a dilute suspension containing porous particles.

A porous particle is modelled by a system consisting of N spherical liquid-impermeable particles with a given packing density. It is assumed that the liquid flow inside the porous particle obeys the Brinkman equations

$$\nabla p = \eta \Delta \boldsymbol{u} - K\boldsymbol{u},$$

where p is the pressure, $\boldsymbol{u}$ is the fluid velocity vector, η and K are the viscosity and the resistance coefficient of a porous medium, respectively.

The solution of this equation gives the following differential equations for the effective suspension viscosity and the resistance coefficient:[57]

$$\frac{d\eta}{d\varphi} = \frac{5}{2}\frac{\eta}{1 - \varphi}, \quad \frac{dK}{d\varphi} = \frac{9\pi}{2R^2}\frac{\eta}{1 - \varphi}.$$

The boundary conditions: $\varphi = 0$, $\eta = \eta_0$ and $K = K_0$, where R is the radius of the porous particles, η_0 and K_0 are the viscosity and the resistance coefficient of the Brinkman fluid free of additional inclusions.

This differential equation system has the following solution:

$$\eta = \eta_0(1 - \varphi)^{-5/2}, \; K = K_0 + \frac{9}{7}\frac{\pi\eta_0}{R^2}\left[(1 - \varphi)^{-5/2} - 1\right].$$

These equations determine the dependece of the effective suspension viscosity and the flow resistance coefficient taking into account the particle permeability to a dispersion medium.

An important class of rheological models includes models that are based on analysis of the processes of formation and cleavage of bonds between the particles. These models are called kinetic models because they are described by kinetic equations that characterise the changes in the bond numbers. The best known model of this type was developed in the study.[58] The kinetic equation for this model is as follows

$$\frac{dN_1}{dt} = -k_1 N_1^n + k_2 N_2^m, \tag{27}$$

where N_1 and N_2 are the concentrations of non-broken and broken bonds, and k_1, k_2, n and m are the constants characterising the rates of destruction and regeneration of the system.

An analogous model was proposed by Stolin *et al.*[59] The authors used a rheological system consisting of the structures A and B and identified the destruction and regeneration of the system with the forward and reverse chemical reactions

$$A \underset{k_2}{\overset{k_1}{\rightleftharpoons}} B$$

The constants k_1 and k_2 are similar in meaning to the analogous parameters in Eqn (27). Their dependence on the shear rate was taken into consideration under the following assumptions:

(i) an increase in the deformation intensity leads to stronger structural changes (up to destruction);

(ii) noticeable structural changes occur after elastic deformation (development of high-elastic deformations).

It is taken that

$$k_1 = k_{10}\exp\left(\frac{\omega}{2k_B T}\right),$$

$$k_2 = k_{20}\exp\left(-\frac{\omega}{2k_B T}\right),$$

where $\omega = (G/\tau)\dot{\varepsilon}^2$ is the energy accumulated during elastic deformation τ.

The equation relating the dimensionless stress $\bar{\sigma}$ and the shear rate $\bar{\dot{\varepsilon}}$ was written in the following form [59]

$$\bar{\sigma} = \frac{\bar{\dot{\varepsilon}}\left(1 + \kappa\exp\bar{\dot{\varepsilon}}^2\right)}{\lambda + \kappa\exp\bar{\dot{\varepsilon}}^2} \tag{28}$$

Here $\bar{\sigma} = F_A\alpha^{1/2}\sigma$, $\alpha = G/\tau$, $\bar{\dot{\varepsilon}} = \alpha^{1/2}\dot{\varepsilon}$, $\kappa = k_{10}/k_{20}$, $\lambda = F_A/F_B$, F_A and F_B are the fluidities of the structures A and B, respectively.

Therefore, the viscosity of a system in the kinetic models is related to the concentrations of broken and non-broken structures (bonds) and it can be estimated from the corresponding kinetic equations.

Equation (28) describes the viscosity superanomaly, *viz*., a decrease in the deformation resistance with increasing shear rate in stationary flows, characteristic of tixotropic structured systems. In this case, the flow curve (the shear rate *vs*. the shear stress) is a multivalued function. Its plot has a lower and upper branches, jumps from one branch to another being possible. This dependence was observed experimentally for various disperse systems and it is associated with the above-discussed discontinuity effect.[41] It should also be noted that an agreement between the experiment and Stolin's model is evidently due to a free choice of a large number of independent parameters.

The kinetic model of aggregation – fragmentation of particles in a hydrodynamic shear flow of a coagulated suspension was developed by Dolgonosov.[60, 61] In the equilibrium state, where the rates of attachment of the particles to aggregates is equal to the detachment rate, a dispersed phase was demonstrated to be separated into two fractions. One fraction consists of large aggregates, whereas another fraction is composed of small particles (initial particles and small aggregates). The formation of a two-fraction pattern was attributed to the fact that the growth of small and larger aggregates occurs by different mechanisms (Brownian and gradient). Within this model, the particles of the small and larger fractions are characterised by continuous spectra of masses $f(\mu)$ and $F(m)$ (μ and m are the particle masses of the corresponding fractions). The functions f and F were each normalised to the number of particles in the corresponding fraction. Under the assumptions used for the description of coagulation of small particles and their uptake by aggregates, as well as of the growth and degradation of aggregates, the following kinetic equations were derived:

$$\frac{\partial f(\mu)}{\partial t} = \int_0^{\mu/2}\beta(\mu-\mu',\mu')f(\mu-\mu')f(\mu')\mathrm{d}\mu' - \tag{29}$$

$$-\int_0^{\infty}\beta(\mu,\mu')f(\mu)f(\mu')\mathrm{d}\mu' - \int_0^{\infty}\beta(m,\mu)F(m)f(\mu)\mathrm{d}m +$$

$$+\int_{\mu}^{\infty}\gamma(m-\mu,\mu)F(m)\mathrm{d}m,$$

$$\frac{\partial F(m)}{\partial t} = \int_0^{m/2}\beta(m-\mu,\mu)F(m-\mu)f(\mu)\mathrm{d}\mu - \tag{30}$$

$$-\int_0^{\infty}\beta(m,\mu)F(m)f(\mu)d\mu + \int_0^{\infty}\gamma(m,\mu)F(m+\mu)\mathrm{d}\mu -$$

$$-\int_{\mu}^{m/2}\gamma(m-\mu,\mu)F(m)\mathrm{d}\mu.$$

Here $\beta(x,y)$ is the kernel of coagulation (the specific rate of coagulation of the particles x and y into the aggregate $x + y$) and $\gamma(x,y)$ is the kernel of degradation (the specific rate of degradation of the aggregate $x + y$ into the fractions x and y). The functional type of the sites of coagulation and degradation is written with consideration for the mechanism of aggregate growth with the use of approaches developed in the studies.[62–65]

Calculations within this model allow one to reveal the changes in the spectrum of particles of a dispersed phase with time (Fig. 5). Analysis of the results of calculations showed that the evolution of the dispersed phase involves three steps: 1) the initial step: as a result of coagulation of aggregates, a coarse fraction manifests itself as several modes in the spectrum, which are transformed into one resulting asymmetric mode upon coalescence; 2) the intermediate step: aggregate coagulation continues, resulting in a decrease in asymmetry of the mode; 3) the final step: aggregation ceases, and ageing of the dispersed phase occurs due to capture of particles of the fine fraction by aggregates and detachment of fragments from aggregates under hydrodynamic stresses.

Calculations demonstrated that the peak in the spectrum of the fine faction decreases in height and is broadened with time. In the studies,[60, 61] it was demonstrated that the fine and coarse fractions do not overlap throughout the process, which is a condition for the applicability of the two-fraction model of a dispersed phase. The cited studies dealt with low-concentration disperse systems, in which the possibility of structuring is excluded, and only the kinetics of the formation of a dispersed phase was calculated taking into account coagulation and fragmentation of the particles. Apparently, the proposed model can be used also in calculations of the rheological characteristics of such systems.

Of the processes that substantially influence the rheological properties of dispersions, immobilisation of a liquid with aggregates and particles deserves notice. A liquid can be immobilised both on the particle surface and within aggregates. The immobilised liquid is not a true component of the liquid phase because it is bound to particles, and this liquid would be more properly considered as an supplement to solid particles, which increase the effective volume concentration of the dispersed phase

$$\varphi_{ef} = \varphi + \varphi_s + \varphi_v,$$

where φ_s and φ_v are the fractions of the liquid immobilised on the particle surface and in the bulk of aggregates, respectively.

The influence of immobilisation of the liquid on the rheological characteristics of suspensions was discussed by Windhab.[66] The volume of the immobilised liquid depends substantially on the degree of aggregation of the system, the particle surface roughness, the viscosity of the liquid, the porosity of aggregates, their density (Fig. 6) and other factors. Deaggregation of the system leads to release of the liquid located between the particles in the aggregate, resulting in a decrease in the volume of the immobilised liquid (φ_{ef}). However, further deaggregation leads to immobilisation of the liquid on the newly formed particle surface resulting in an increase in φ_{ef}. The effective concentration φ_{ef} directly affects the suspension viscosity. Therefore, the viscosity of the system

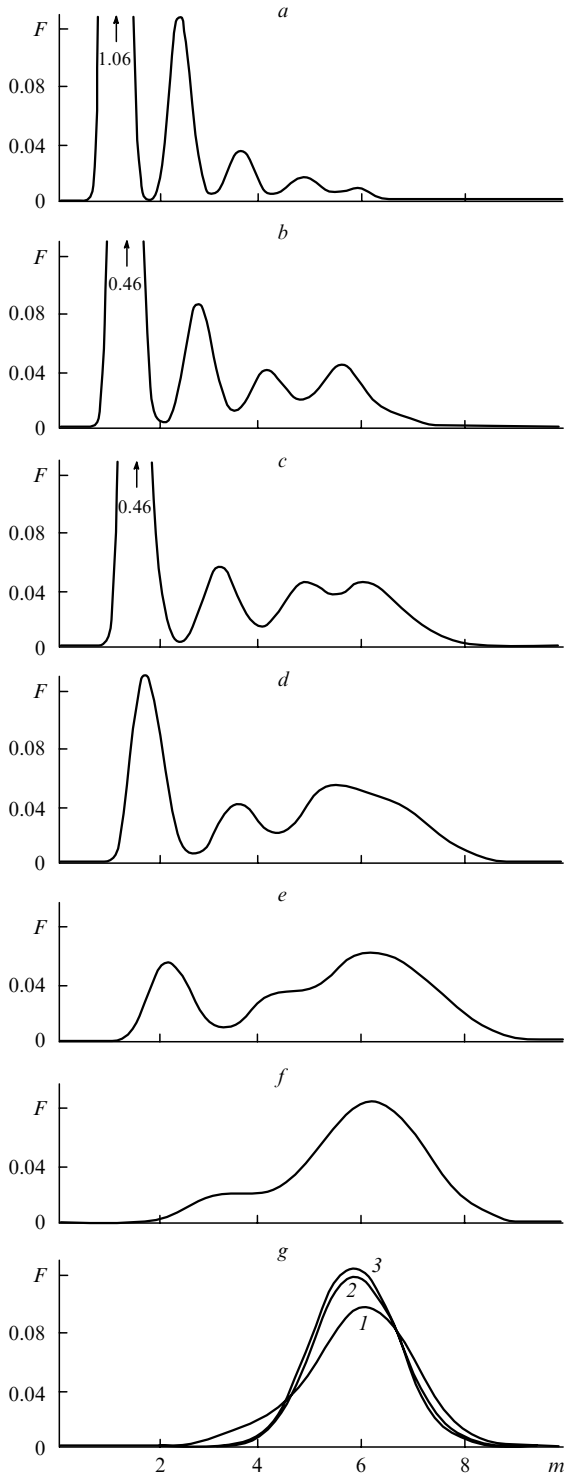


Figure 5. Mass distribution density of large aggregates *vs*. the time (t).[61] t = 0.1 (*a*), 0.2 (*b*), 0.3 (*c*), 0.4 (*d*), 0.6 (*e*), 1.1 (*f*), 1.5 (*g*, curve *1*); 7.0 (*g*, curve *2*); *3*, the Gaussian approximation of the equilibrium distribution; t is a dimensionless value.

changes with a change in the shear rate resulting in the aggregation or deaggregation and immobilisation or release of the liquid.

The following equation for the effective volume concentration was obtained:[66]

$$\varphi_{ef} = \varphi\left\{1 + \frac{1-\varphi_m}{\varphi_m}\left[1 + (\psi - 1)\frac{3}{4}n^{-1/3}\varphi_m^{1/3}\right]\right\}. \qquad (31)$$

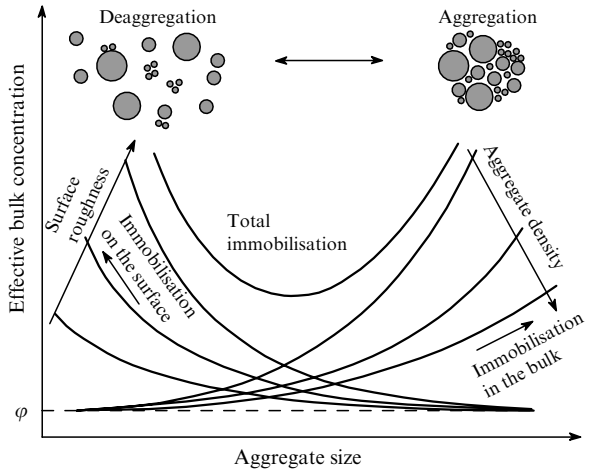


Figure 6. Degree of immobilisation of the liquid on the surface and in the bulk of particles or aggregates as a function of aggregability of the system.[66]

Here $\psi = \Delta V_s/\Delta V_v$ is the ratio of the volume increments of the liquid immobilised on the surface (ΔV_s) and in the bulk (ΔV_v) of aggregates due to aggregation (deaggregation) of the system and n is the number of particles in the aggregate. Aggregation can lead to either a decrease or increase in the viscosity depending on ψ (at $\psi > 1$ and $\psi < 1$, respectively).

The number of the particles in the aggregate is calculated according to the equation

$$n = n(0)\left\{\frac{k_a + k_d \exp[-(k_a + k_d)t]}{k_a + k_d}\right\}, \qquad (32)$$

where $n(0)$ is the number of particles at the initial point of time and k_a and k_d are the rate constants of aggregation and deaggregation, respectively.

In the study,[66] it was suggested that Eqns (31) and (32) combined with the Krieger–Dougherty equation (4) be used for the estimation of the suspension viscosity:

$$\eta(\varphi, \dot{\varepsilon}, t, \delta) = \eta_0\left[1 - \frac{\varphi_{ef}(\varphi, \dot{\varepsilon}, t, \delta)}{\varphi_m}\right]^{-\alpha(\delta)\varphi_m}. \qquad (33)$$

The additional parameter δ takes into account the influence of the orientation of aspherical particles in a flow.

A comparison of the results of calculations according to Eqn (33) with experimental data showed that the model gives underestimated viscosities (Fig. 7). Apparently, this can be attributed to the fact that this model does not take into consideration the microstructure formation, which affects the viscosity of disperse systems.

The microrheology of low-concentration fractal colloidal gels was documented in several publications.[67–74] If the shear stress applied to such gels is small, the gels exhibit 'solid-like' properties, *viz*., a high viscosity and the modulus of elasticity at low frequencies. If the stress is higher than the threshold value, the viscosity and, in some cases, the modulus of elasticity fall by several orders of magnitude and the system exhibits 'liquid-like' properties. An explanation of the nature of solid- and liquid-like states was given in the studies.[67, 68] It was assumed that, at stresses higher than the threshold value ($\sigma > \sigma_c$), the structure consists of fractal aggregates, which are in contact with each other but are not linked in a network, and the system exhibits liquid-like properties. At $\sigma < \sigma_c$, the system occurs in the gel state, *i.e*., it consists of aggregates linked in a network and exhibits solid-like properties.

For the solid-like state, the viscosity can be estimated according to the equation [67, 73]

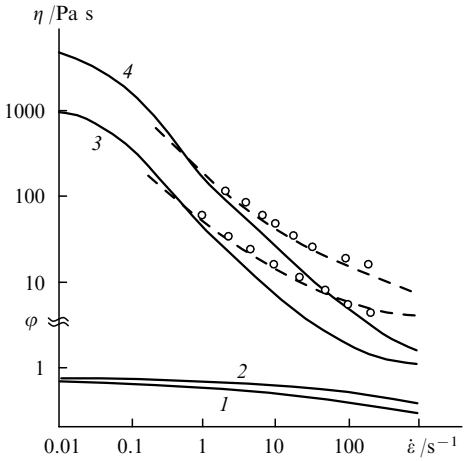


Figure 7. Calculated (solid curves) and experimental (points) dependences of the shear viscosity of a sugar dispersion in silicon oil.[66]
The results of approximation of experimental points by polynomials are indicated by dashed curves.
(*1*) φ_{ef} at $n_0 = 1000$; (*2*) φ_{ef} at $n_0 = 5000$; (*3*) η at $n_0 = 1000$; (*4*) η at $n_0 = 5000$; (n_0 is the number of particles in the aggregate in the absence of shear).

$$\eta_s \cong \alpha G_0 \tau_0 \exp\left(\frac{E}{k_B T}\right) c^{(3+2f_r)/(3-f_a)}. \quad (34)$$

Here $\alpha < 1$ is the coefficient that takes into consideration a decrease in the shear modulus in the space between the particles, G_0 is the shear modulus of the material of colloidal particles, τ_0 is the period of thermal oscillations of a pair of bound particles, E is the bond energy of the particles, c is the volume concentration of the particles in the system $c = c_N d^3$ (c_N is the numerical concentration of colloidal particles), f_r is the fractal dimensionality of unreplicated bonds in the backbone of the aggregate and f_a is the fractal dimensionality of the aggregates.

The viscosity of a gel in the liquid-like state is

$$\eta_f \cong B\pi\eta_0, \quad (35)$$

where $B > 1$ is the coefficient that takes into account the asphericity of the aggregate.

The critical (threshold) stress is

$$\sigma_c = K\frac{p_c E}{\xi^3}, \quad (36)$$

where $K \approx 1$ is the coefficient, p_c is the critical fraction of broken bonds, which is determined based on the percolation concepts, for a three-dimensional problems $p_c \approx 0.6-0.8$, and ξ is the linear size of the aggregate.

In the study,[67] it was concluded that at $\sigma = \sigma_c$, the system is inhomogeneous and stratifies into two phases, which are characterised by the viscosities η_s and η_f and the shear rates σ_c/η_s and σ_c/η_f. The shear rate changes stepwise with height. In regions corresponding to solid-like layers, the shear rate is lower than the average rate, whereas it is higher than the average rate between the layers.[74]

The possibility of the co-existence of solid-like and liquid-like layers in a shear flow of low-concentration colloidal gels was considered in detail.[72, 74] In those studies, the co-existence of the layers in a shear flow in the shear rate range $\sigma_c/\eta_s \leqslant \dot{\varepsilon} \leqslant \sigma_c/\eta_f$ was demonstrated to be responsible for the minimum energy dissipation rate, *i.e.*, the presence of these layers is energetically favorable. The fraction of the cross-section, which is perpendicular to the sample flow and is occupied by liquid-like layers, is determined by the equation

$$\varphi_f = \frac{\dot{\varepsilon}/\sigma_c - 1/\eta_s}{1/\eta_f - 1/\eta_s}. \quad (37)$$

An idea of the co-existence of solid- and liquid-like phases was extended to gels under periodic shear deformation.[68] In the publication,[71] the theoretical views about the structures of low-concentration gels were used for the description of the state of such gels under shear compression. In particular, it was noted that compression can lead to contacts between the branches (formed by particles) attached to the backbones of fractal cells and their gluing, on the one hand, and the cleavage of the most burdened branches, on the other hand.

The criterion formulated in the study [69] allows one to predict whether aggregates can fill the volume of the system and form a gel. This criterion is based on parameters of dilute colloidal systems in which fast coagulation of particles occurs and non-equilibrium fractal aggregates are formed. If the gel formation does not occur, aggregates fill a small volume fraction of the system, and their average sizes remain virtually unchanged with time because aggregation is compensated by fragmentation of aggregates (a stationary state). The volume concentration of the particles in the system was taken to be small, the aggregates were considered as consisting of a large number of particles, and the scaling solution of the Smoluchowski equations for large stationary aggregates, which was obtained earlier,[75] was used. The Smoluchowski equations include only pair collisions of aggregates and these equations are approximate, when the volume fraction occupied by aggregates φ_a is large.

In the case of formation of stationary fractal aggregates, their characteristics are described by the following expressions:
the weighted-average mass of aggregates

$$M \cong \left(c_N \frac{k}{f}\right)^{1/(2+\beta-\alpha)}; \quad (38)$$

the average aggregate size

$$R \cong dM^{1/f_a} \cong d(cAn)^{(1/f_a)/(2+\beta-\alpha)}; \quad (39)$$

the number of aggregates per volume unit

$$n \cong \frac{c_N}{M} \cong d^{-3}c(cAn)^{-1/(2+\beta-\alpha)}; \quad (40)$$

the volume fraction occupied by aggregates

$$\varphi_a \cong nR^3 \cong c(cAn)^{(1/f_a)/(2+\beta-\alpha)}; \quad (41)$$

the time of establishment of a stationary state

$$\tau \cong \frac{d^3}{ck}(cAn)^{(1-\alpha)/(2+\beta-\alpha)} \cong \frac{1}{f}(cAn)^{-(1+\beta)/(2+\beta-\alpha)}. \quad (42)$$

Here k and f are the coagulation and fragmentation constants, respectively, α and β are the parameters that characterise the homogeneity upon coagulation and fragmentation, respectively, d is the particle size, f_a is the fractal dimensionality of the aggregates and $An = d^{-3}k/f$ is the dimensionless parameter that characterises the ability of the system to undergo aggregation.

In the case of fast Brownian aggregation in the absence of cyclic (closed) fragments in the structure of fractal aggregates, the parameters α and β are equal to zero. Taking $f_a = 2$, the criterion of the existence of a gel can be obtained from Eqn (41) as the condition $\varphi_a \cong 1$ (aggregates fill the total volume).

$$c^{5/4}(An)^{1/4} \cong 1. \quad (43)$$

The region of the parameters c and An, at which the aggregates are not linked to each other and exist in a stationary state, is shown in Fig. 8. This region is limited by the weighted-average mass of the aggregates $10^2 < M < 10^6$. The requirement of large aggregate masses is associated with the fact that fractal models are

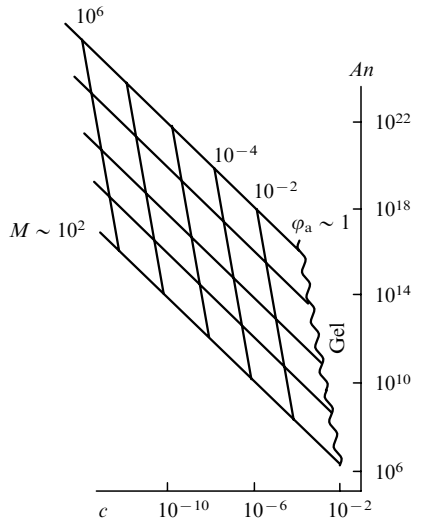


Figure 8. Region of the existence of stationary aggregates (without cyclic fragments) on the coordinates particle volume concentration – aggregability of the system.[69]
The region is bounded by the straight lines $M = 10^2$ and 10^6. The region of the existence of a gel is on the right from the wavy line.

adequate only in this case. However, the mass of real fractal aggregates cannot be much larger than 10^6, because their structure will be substantially deformed under gravitation and thermal fluctuations. The wavy line in the Figure corresponds to the boundary of the gel formation $\varphi_a \sim 1$.

It should be noted that aggregates occupy virtually the whole volume of the system at $\varphi_a \sim 1$. In this case, the gel formation is beyond doubt. At the same time, the gel formation can occur at lower concentrations as well. The approximate character of the above criterion is associated also with the fact that the Smoluchowski equation that lies at the basis of this criterion is valid (as mentioned above) only at low φ_a.

3. Suspension dynamics under vibration in the presence of surfactants

A decrease in the viscosity of disperse systems (an increase in their fluidity) is one of the main conditions of optimisation of many heterogeneous chemical engineering processes. This problem is of particular importance for highly disperse systems with a high concentration of a solid phase, which are used in virtually all important industrial processes. The viscosity can be decreased by increasing the shear rate, which leads to decoagulation. However, high fluidity of disperse systems can be achieved also at low shear rates, if the dynamic state is created under other external forces, for example, under vibration, particularly, in the presence of surfactants.

The results of vibration treatment are in many aspects similar to the effect of Brownian motion, which hinders the formation of a coagulation structure from particles, thus providing aggregation stability of disperse systems. Vibration induces dispersion of structures. Hence, the vibration effect is analogous to lyophilisation of the system. However, it differs from the Brownian motion in that its parameters can be changed by many orders of magnitude, whereas the only controlled parameter of the Brownian motion, *viz*., the temperature, can be varied only within an order of magnitude.

Experimental vibrorheological curves represent plots of the effective suspension viscosity *vs*. the vibration intensity[39] analogous to usual rheological curves $\eta_{ef}(\dot{\varepsilon})$. Approaches to the theoretical analysis of vibrorheological curves were covered in the monograph.[5]

Within the model of a homogeneous structure, the effective viscosity of a disperse system is calculated according to the equation[5]

$$\frac{\eta_{ef}}{\eta_0} \sim \frac{(\xi\tau_i/\tau_f)^{1/2}\exp(U_a/\theta)}{(1+\tau_f/\tau_i)^{1/2}-(\tau_f/\xi\tau_i)1/2}, \tag{44}$$

where $\xi = h_1/d$, h_1 is the effective range of surface forces, τ_i and τ_f are the characteristic relaxation times of inertial motion of particles and their interaction due to the surface forces, U_a is the potential energy of particle interactions and θ is the parameter that characterises the kinetic energy of chaotic motion of particles.

For the suspensions considered in the monograph,[5] $\tau_f \gg \tau_i$. In this case, Eqn (44) takes a simple form

$$\frac{\eta_{ef}}{\eta_0} \sim \exp\left(\frac{U_a}{\theta}\right). \tag{45}$$

When Eqns (44) and (45) are applied to suspensions under vibration conditions, the parameter θ includes, along with the energy of thermal motion of particles, the energy imparted to the particles under vibration,

$$\theta = k_B T + m(A\omega)^2,$$

where A and ω are the vibration amplitude and frequency, respectively.

At rather high θ (high vibration intensity), destruction occurs to give aggregates. In this case, models of aggregated suspensions can be used in the vibrorheological analysis of disperse systems.

The equations for the viscosity of low-concentrated aggregated suspensions with a fractal structure can be derived based on the concepts of sedimentation stability of suspensions by replacing the acceleration of gravity g by the acceleration produced by vibration $A\omega^2$. The following equations for the viscosity under vibration were thus obtained:[5]

within the mean-field model

$$\frac{\eta_{ef}}{\eta_0} = \left[1 - \frac{\varphi}{\varphi_m^2}\left(\frac{1.1}{\xi_v}\right)^{\sigma(3-f)/(f-1)}\right]^{-1.5}; \tag{46}$$

within the lubrication model

$$\frac{\eta_{ef}}{\eta_0} = \frac{6.2}{\xi_v}\left(\frac{\varphi}{\varphi_m^2}\right)^{\gamma_1[(3-f_r)+(f-2)]/(3-f)}. \tag{47}$$

Here

$$\xi_v = \frac{2}{9}\frac{|\rho-\rho_0|dA\omega^2}{\sigma_{0v}},$$

σ_{0v} is the resistance to vibration $\sigma_{0v} = \kappa\sigma_0$, $\kappa \ll 1$, f is the fractal dimensionality, σ_0 is the stability of the structure in the absence of vibration

$$\sigma = \frac{f-1}{(3-f)\gamma_1 + (f-2)} = \frac{f-1}{1+f(1+1/f_r)},$$

$f_r = f/f_c$, f_c is the chemical dimensionality;[76,77]

$$\gamma_1 = \frac{2\alpha}{(3-f)(f-1)},$$

α is the parameter that depends on the degree of anisometry of the cluster, $0 \leqslant \alpha \leqslant f-1$.

The viscosity of highly concentrated suspensions can be estimated from the equation

$$\eta_{ef} \approx 17\eta_{ext}\left[\frac{\varphi_m-\varphi}{1-\varphi_m}\frac{|\rho-\rho_0|RA\omega^2}{\kappa\sigma_0} + \left(\frac{\eta_{ext}\dot{\varepsilon}}{\sigma_0}\right)^{1/2}\right]^{-1}, \tag{48}$$

where

$$\eta_{ext} \equiv \frac{9}{8}\frac{\eta_0}{(\varphi_m/\varphi_{ext})^{1/3}-1},$$

η_{ext} and φ_{ext} are, respectively, the viscosity and concentration of the suspension that fills the space between aggregates.

At low shear rates $\dot{\varepsilon}$, Eqn (48) takes the form

$$\frac{\eta_{ef}}{\eta_{ext}} \approx 17\frac{1-\varphi_m}{\varphi_m-\varphi}\,\frac{\kappa\sigma_0}{|\rho-\rho_0|RA\omega^2}. \qquad (49)$$

The influence of the particle surface modification with surfactants can be taken into account by varying the parameters U_a, h_1 and κ in Eqns (44)–(49).

Analysis of the resulting equations and their comparison with experimental data showed that the plot of the viscosity η_{ef} *vs.* the vibration intensity $I = A^2\omega^3$ is characterised by the presence of the following two regions. At small values, the viscosity is calculated according to Eqns (44) and (45). At large values, the viscosity is calculated from to Eqns (48) and (49). These regions are associated with different flow mechanisms: a flow with a continuous structure (a model of a homogeneous structure) and degradation of the structure into aggregates and individual particles (a model of finite aggregates). In the former case, the viscosity decreases exponentially with increasing vibration intensity due to destruction of a homogeneous system. In the latter case, a weaker (power) dependence is observed, which corresponds to the aggregation mechanism of destruction. Since the viscosity depends on $A\omega$ and $A\omega^2$ in the first and second segments of the curve, respectively, it is reasonable to use relatively low-frequency vibrations to perform destruction in the initial step, whereas higher-frequency vibration must be used to achieve deeper destruction giving rise to aggregates. Vibration makes it possible to eliminate the segment of abnormally high viscosities at low shear rates in the rheological curve, in particular, to provide fluidity at shear stresses much lower than the effective yield point.

The influence of orthogonal oscillations on a disperse system (chocolate, $T = 32$ °C) under shear is shown in Fig. 9.[78] Measurements were performed on a MCR-500 rotational rheometer. The experimental data showed that the viscosity substantially decreases in a wide range of shear rates.

The addition of surfactants to disperse systems reduces the lyophilic–lyophobic surface mosaicity of particles and favours a decrease in the viscosity in all regions, the general view of the rheological curve remaining unchanged (Fig. 10). Analysis of the dependences presented in Figs 9 and 10 revealed the effect of vibro-dilatancy consisting of the increase in the viscosity with increasing shear rate under vibration. The mechanism of this effect associated with the change in the structure of the flow remains unclear.

A high degree of deformation homogeneity can be achieved using vibration along with a decrease in the viscosity of a structured suspension due to 'healing' of discontinuities.[41] Hence, vibration (particularly, combined with the addition of surfactants) can be considered as a universal tool for controlling the rheological properties of disperse systems.

An interesting synergism was observed under the combined action of different types of vibrations and surfactants on disperse systems. It was demonstrated[79] that low-frequency mechanical vibrations combined with high-frequency ultrasonic vibrations (60 Hz and 22 kHz, respectively) provide a higher degree of microstructure homogeneity of experimental samples (epoxy-based composite materials were examined as the samples). The possibilities of controlling the properties of disperse systems with the use of surfactant mixtures are much wider than those with individual surfactants. The colloid-chemical properties of aqueous solutions of high- and low-molecular-weight surfactants, *viz.*, proxanol 228 and sodium alkylbenzenesulfonate, respectively, and their 1 : 1 mixture were investigated.[80] The surfactant properties of the mixture were demonstrated to be more pronounced than the properties of the individual surfactants. Besides, the use of the mixture ensures higher aggregation stability of the system. Therefore, a combination of high- and low-molecular-weight surfactants results in the effect that is not observed in the case of individual surfactants.

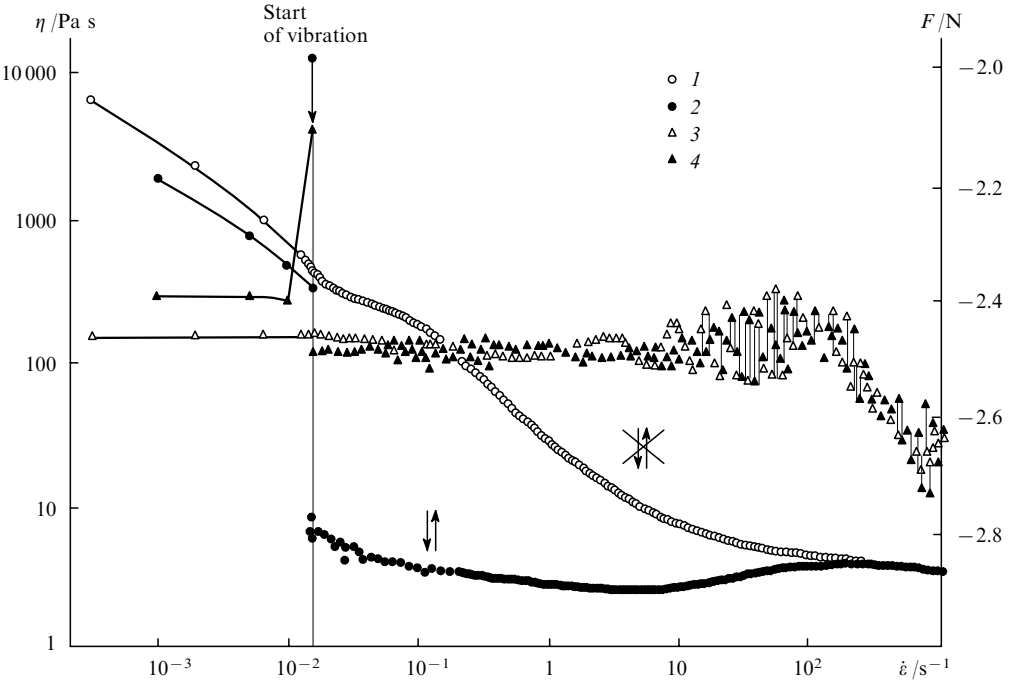


Figure 9. Changes in the shear viscosity (*1*, *2*) and the normal force (*3*, *4*) (chocolate, $T = 32$ °C, a MCR-500 rotational rheometer) under orthogonal oscillations.[78]
(*1*, *3*) Without vibration; (*2*, *4*) under vibration ($\nu = 60$ Hz, $A = 0.5$ mm).

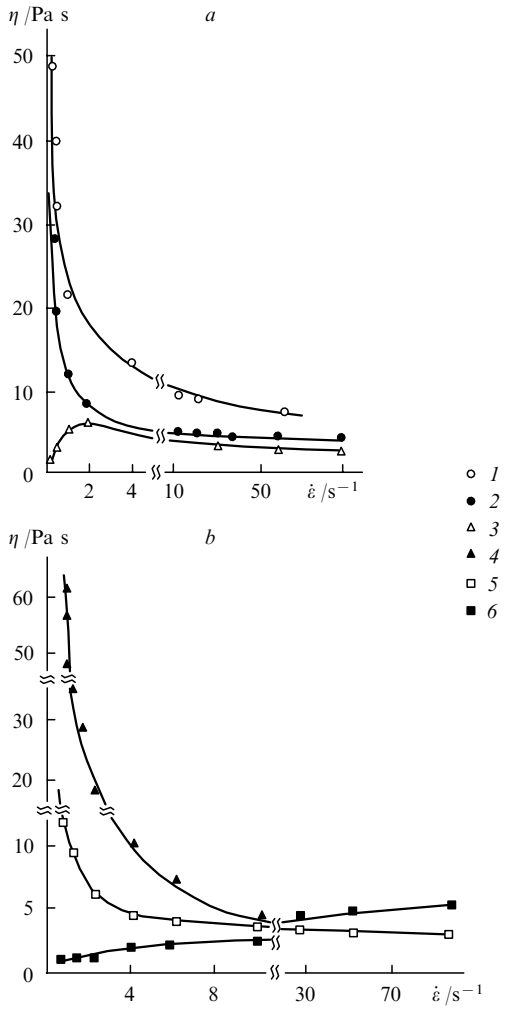


Figure 10. Changes in the rheological curves of water–coal suspensions in the presence of surfactants and under vibration based on brown coal from the Moscow Coal Basin with $\varphi = 41\%$ (*a*) and thermal coal from the Belovskii deposit with $\varphi = 72.5\%$ (*b*).[3]
(*1*, *4*) In the absence of surfactants; (*2*) in the presence of potassium lignosulfonate (0.4%); (*3*) in the presence of potassium lignosulfonate combined with vibration, $\nu = 50$ Hz, $A\omega^2 = 10g$; (*5*) in the presence of the condensation product of naphthalenesulfonic acid and formaldehyde (1%); (*6*) with the same additive as that used in *5* combined with vibration, $\nu = 50$ Hz, $A\omega^2 = 2.5g$.

The resistance of structured disperse systems to vibration and the knowledge of conditions under which destruction becomes impossible are of considerable importance. These problems were examined [81] by analysing vibrations of a particle caused by oscillations of the fluid in a potential well in the vicinity of an equilibrium state. The equation for forced vibrations of a particle oscillator near equilibrium takes the form [82]

$$\frac{\partial^2 x_{ij}}{\partial t^2} + 2\lambda_i \frac{\partial x_{ij}}{\partial t} + \omega_i^2 x_{ij} = \frac{F_j}{m} \sin \omega t, \tag{50}$$

where x_{ij} is the displacement of the particle from the equilibrium position, $i = 1$ and 2 correspond to the long- and short-range coagulation, respectively, $j = 1$ and 2 correspond to different calculation methods of the force F_j, $\lambda_i \sim z\eta_0 r^2/(H_i m)$, z is the coordination number, r is the particle radius, H_i is the distance which corresponds to the long- and short-range coagulation, m is the particle mass and ω_i is the eigenfrequency of vibrations of the particle.

The law of forced vibrations of a particle was derived from the equation of motion (50) [82]

$$x_{ij}(t) = b_{ij} \sin(\omega t + \psi_i),$$

where

$$b_{ij} = \frac{F_j}{m\left[\left(\omega^2 - \omega_i^2\right)^2 + \lambda_i^2 \omega^2\right]^{1/2}},$$

ψ_i is the phase difference between the vibrations of the particle and the fluid.

The particle can escape from a potential well when exposed to the force F_j, if one of the following inequalities is fulfilled:[81]

$$b_{ij} \gg H_i, \tag{51}$$

$$m b_{ij}^2 \omega^2 \gg U_i. \tag{52}$$

If inequality (51) is fulfilled, the particle will be displaced from the equilibrium position to a distance larger than the potential well width, *i.e.*, will go beyond the range of action of the surface forces. If inequality (52) is fulfilled, the particle will acquire an energy higher than the potential well depth U_i and move as though there were no surface forces, $\omega_i = 0$. In both cases, the particle breaks free of the bonds that hold it in the structure, *i.e.*, destruction occurs. Detailed analysis of the particular form of conditions (51) and (52) for various modes of estimation of the force F_j as applied to long- and short-range coagulation, respectively, was performed in the study.[81]

In the case of destruction of structured systems that hinder high fluidity of dispersions the inertial effects are of importance in achieving the isotropic dynamic state of solid/liquid (S/L) disperse systems. When moving in an oscillating fluid, the vibration amplitude of the particle does not necessarily coincide with the vibration amplitude of the fluid. This effect becomes more pronounced as the particle mass increases, the oscillation frequency of the fluid increases or the viscosity of the fluid decreases. Under steady-state vibration mode, the proportionality coefficient β between the vibration amplitudes of the fluid (A) and the particle (A_p)

$$A_p = \beta A$$

is calculated according to the equation [83]

$$\beta = \frac{\lambda}{\left(1 + \lambda^2\right)^{1/2}},$$

where

$$\lambda = \frac{9\eta_0}{\pi d^2 \rho \nu},$$

ν is the vibrational frequency of the liquid in Hz.

The coefficient β is essentially the criterion that indicates whether destruction and deaggregation can occur in a suspension. Destruction can take place if the particles that form the system are characterised by different values of coefficient β. The wider is the range of variations in β, the faster and more efficient is destruction. This condition means that only polydisperse systems with a wide range of variations in the particle size can undergo destruction in a suspension of rigid spheres under vibration. In this case, particles with different masses oscillate with different amplitudes due to which the particles are displaced with respect to each other resulting in destruction.

It should be noted that A_p are the amplitudes of free (*i.e.*, non-interacting) particles. The real amplitudes can be lower than A_p if there are interactions between the particles. This means that the above criterion provides evidence only for the possibility of destruction of structured components. Structural stability determined by interparticle forces is responsible for whether or not destruction will occur. To overcome these forces, it is necessary that the energy supplied under vibration be sufficient for cleavage of coagulation contacts [see Eqns (51) and (52)]. In other words,

this criterion describes the conditions necessary but insufficient for destruction of S/L disperse systems.

Undoubtedly, destruction and deaggregation under vibration depend on the degree of anisometry of the particles involved in the structures and aggregates. The value and character of the hydrodynamic forces acting on the particles depend substantially on their shape. At high anisometry, not only relative displacements of particles but also their more complicated translational-rotational motions take place resulting in faster deaggregation.

It is known that the presence of a surfactant layer on the particle surface leads to an increase in aggregation stability of disperse systems due to high viscosity, mechanical strength of the absorption layer and lyophilicity of its outer surface. Based on these facts, the structural-mechanical barrier is considered as one of factors stabilising disperse systems under static conditions.[34, 84] However, stability of systems under dynamic conditions is of particular importance and there is a need for a theoretical description of the parameters and prerequisites for the appearance of the structural-mechanical barrier in the dynamic state. The processes that occur in adsorption layers on the surface of the particles during their high-speed collisions were analysed.[85] The layers are characterised by the viscosity coefficient η_l and the modulus of elasticity E_l. It was noted that the breakdown of an adsorption layer can take place at a rather high velocity of approach of particles to each other V_s. The breakdown occurs if the mechanical stress in the layer is comparable to the strength of the layer p_l. The inertial breakdown, *i.e.*, the breakdown due to the kinetic energy of particles received from an external source, was considered. Under these conditions, the viscous properties of the layer at particle velocities close to breakdown values can be ignored because the collision time is much shorter than the relaxation time (the time of elastic after-effect) $\tau_r \sim \eta_l/E_l$. In this case, the layer behaves as a purely elastic layer.

A quantitative expression for the criterion for the layer breakdown can be derived by comparing the kinetic energy $\Delta\varepsilon_k$, which is received by particles from an external source, with the sum of the elastic energy $\Delta\varepsilon_{ei}$, which can be accumulated in the layer without destruction, and the energy $\Delta\varepsilon_{hi}$ dissipated for viscous friction as the surfaces approach each other.

The breakdown criterion is determined by the inequality

$$\Delta\varepsilon_k > \Delta\varepsilon_{ei} + \Delta\varepsilon_{hi}. \tag{53}$$

According to the results of the study,[85] the terms in this inequality can be estimated according to the formulas

$$\begin{aligned}
\Delta\varepsilon_k &\sim \frac{2\pi}{3} r^3 \rho V_s^2, \\
\Delta\varepsilon_{e1} &\sim E_l L^2 r_1 \left(\frac{p_l}{E_l}\right)^3, \\
\Delta\varepsilon_{e2} &\sim E_l L^2 r_2 \left(\frac{p_l}{E_l}\right)^3 \left(\frac{r}{r_2}\right)^{3/2}, \\
\Delta\varepsilon_{hi} &\sim \int_L^{h_{0i}} F_i \mathrm{d}h.
\end{aligned} \tag{54}$$

Here $r = [3m/(4\pi\rho)]^{1/3}$ is the linear size of anisometric particles (m is the particle mass and ρ is the particle density), L is the thickness of the adsorption layer, r_1 is the local curvature radius of the particle surface for angular collisions ($i = 1$), r_2 is the curvature radius of the lateral surface of disk-like particles ($i = 2$), h_0 is the initial distance between the particles and F_i is the hydrodynamic drag force when the particles approach each other

$$F_i \approx 6\pi\lambda_i\eta_0 \frac{Vr_i^2}{h}, \tag{55}$$

where $\lambda_1 = 1$, $\lambda_2 = 2(r/r_2)^{3/4}$.

Using relations (54) and (55), let us rewrite the criterion (53) as follows

$$V_s^2 - 9\frac{\eta_0}{\rho r}\left(\frac{r_i}{r}\right)^2 \lambda_i \ln\left(\frac{h_{0i}}{L}\right) V_s - \frac{E_l}{2\rho}\left(\frac{L}{r}\right)^2 \frac{r_i}{r} \lambda_i^2 \left(\frac{p_l}{E_l}\right)^3 > 0. \tag{56}$$

This expression corresponds to the general criterion for the loss of aggregation stability under dynamic conditions. The structural-mechanical barrier is an essential factor of stability of dynamic systems, if the thickness of the layer and its modulus of elasticity are rather large. At low values of these parameters, particles are prevented from approaching each other only by hydrodynamic forces, and the minimum breakdown velocity of the layer is independent of the thickness and the modulus of elasticity of the layer.

Inertial coagulation is most probable for anisometric particles, *i.e.*, the creation of a structural-mechanical barrier in dynamics can be used as an efficient way of stabilising real disperse systems. It should be noted that the electrostatic factor is of lesser importance in dynamic systems compared to static systems.[86]

In Section II, we have reviewed the most widely used rheological models of S/L disperse systems and some conclusions and criteria that are based on theoretical analysis of these models. However, the dynamic properties of disperse systems cannot be studied only by analytical methods because of their complexity. It is necessary to use calculation methods and computer simulation to understand the true mechanisms of many phenomena under particular conditions. Below we consider such methods, discuss the possibilities of computer simulation of disperse systems and summarise most characteristic results obtained with the use of these methods.

III. Computer simulation of disperse systems

1. Computer simulation methods for disperse systems

Let us consider approaches to computer simulation of disperse systems at different length scales and the corresponding numerical methods.

Three most important length scales are used in studies of colloidal suspensions (Fig. 11): the microscopic or atomic-molecular level, the mesoscopic level characterised by lengths of the order of colloidal particle size and the macroscopic level where suspensions are considered as a homogeneous fluid. Since the length scales corresponding to these levels differ by several orders of magnitude, it is impossible to perform simultaneous simulation of a suspension at all levels. Each simulation method is, as a rule, intended for the use at a particular level.

Simulations at the atomic-molecular level are carried out with the use of the molecular dynamics method (non-equilibrium molecular dynamics), in which the trajectories of the motion of molecules are calculated taking into account intermolecular forces based on Newton's laws. This method was developed about 50 years ago and was considered in numerous publications (for example, the description of this method has been given in the publications [88–95]). However, the molecular dynamics method is very time consuming. To perform relatively reliable calculations of the fluid bulk properties with the use of this method, it is necessary to simulate systems containing more than 10^9 particles.[91]

The Monte Carlo method can serve as an alternative to the molecular dynamics method in simulations of equilibrium states of systems. The characteristic feature of the Monte Carlo method is its stochastic nature (strictly deterministic equations are used in the molecular dynamics method). In simulations of multiparticle systems, various modifications of the Monte Carlo method are used.[95–100] The essence of the simplest modification is that all particles of the system are alternately subjected to random displacements. After each displacement, the system is tested to ensure whether the whole system satisfies a particular criterion and, if not, a new random displacement is done. After a rather large number of steps, the method gives an equilibrium configuration of particles, which best satisfies the desired criterion (the total energy of the system is generally used as this criterion).

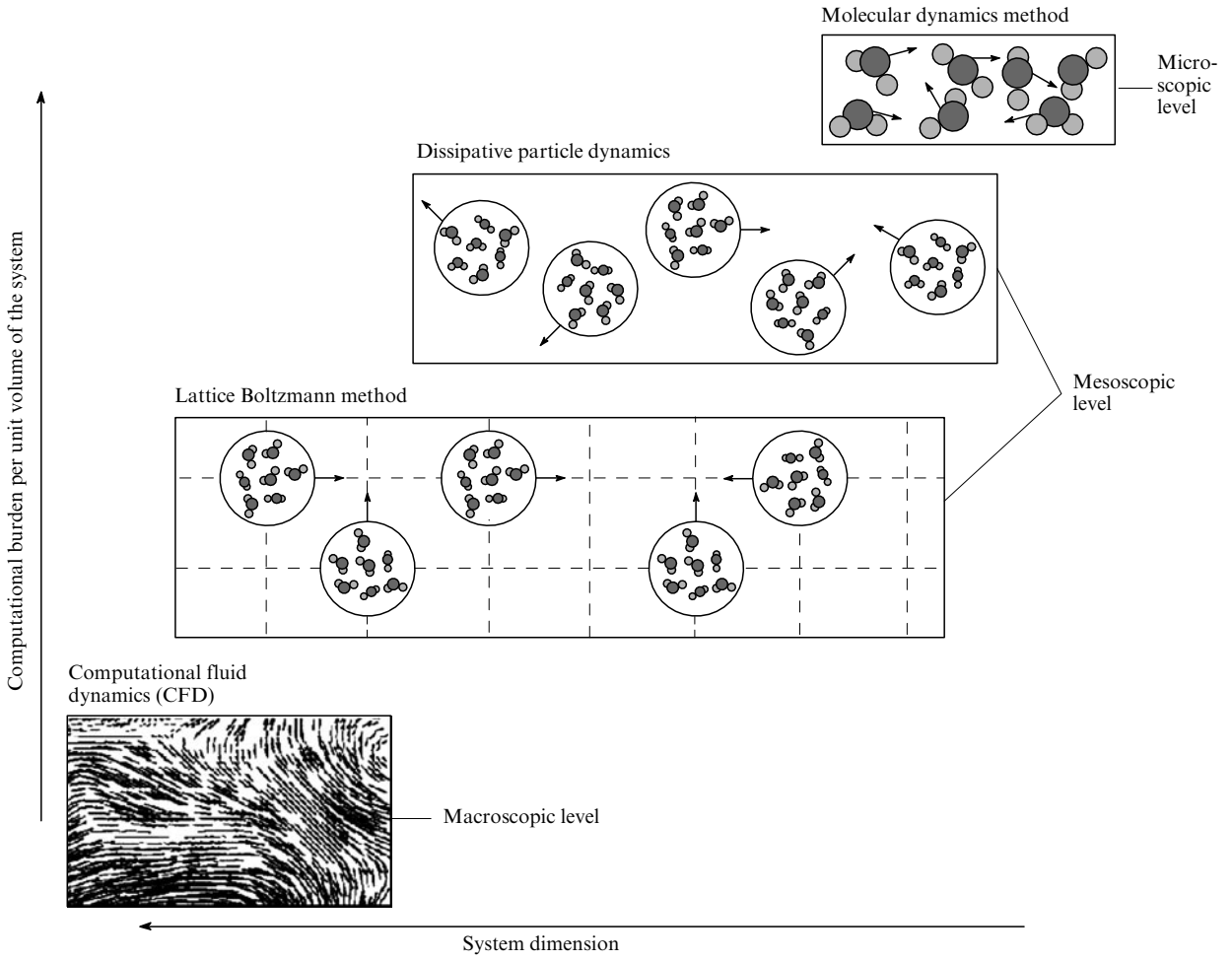


Figure 11. Scheme illustrating the applicability of different approaches to computer simulation of disperse systems at different length scales and the numerical methods used.[87]

Although the Monte Carlo method works faster than the molecular dynamics method, it is unlikely that this method can be used for the description of dispersion flows because it completely ignores the dynamics of the system under consideration.

It is difficult to simulate the behaviour of dispersed particles suspended in a medium of fluid molecules by the molecular dynamics method because it requires a large volume of calculations. To calculate the motion of even one dispersed particle, it is necessary to take into consideration collisions of this particle with at least several thousand 'background' molecules. Moreover, the time of particle–molecule collisions τ_{pm} ($\sim 10^{-9}$ s) is several orders of magnitude shorter than the time of particle–particle collisions τ_{pp} ($\sim 10^{-4}$ s). This means that detailed simulation of a suspension consisting of at least 1000 particles for a time much longer than τ_{pp} requires the use of a giant number of model units and an unrealistic number of iterations.

Brady has demonstrated [101] that the time required for calculations of particles suspended in a fluid with the use of this method increases proportionally to the sixth power of the ratio of the particle size to the molecule size. Even for nanoparticles the sizes of which are larger than those of the fluid molecules by only a factor of 10, the time consumed for calculations increases billionfold. Nevertheless, if simulations are performed for a period of time comparable to τ_{pp}, the use of this method, though being time consuming, is practically possible. However, in most cases, information on the motion of each fluid molecule seems to be excessive in simulation of suspensions because the parameters of the behaviour of particles in suspensions are determined primarily by the macroscopic characteristics of the medium (viscosity, density, flow rates, *etc.*). In this connection, simulations are performed with the use of a continuous homogenous medium with specified macroproperties instead of the fluid molecules. In this case, interactions between particles are determined not only by molecular attraction and electrostatic repulsion but also by hydrodynamic forces transmitted through the fluid.

For small particle sizes (< 1 μm), thermal fluctuations of fluid molecules cause Brownian motion, which, after the replacement of fluid molecules by a continuous medium, can be represented as the result of action of a random force that obeys particular statistical regularities (Brownian dynamics [102–104]). Since the motion of particles generally occurs at low Reynolds numbers ($\mathrm{Re} = \rho d\upsilon/\eta_0 \ll 1$, where υ is the velocity of particles), hydrodynamic interactions are described by the linearised Navier–Stokes equations known simply as the Stokes equations. The corresponding simulation method is called the Stokesian dynamics.[105–107] This method is used for suspensions of particles with a wide range of sizes (10^{-8}–10^{-3} m). The only limitation is that the sizes of dispersed particles should be larger than the sizes of fluid molecules to an extent that the medium can be considered as continuous, and the Reynolds number should be low.[101]

A family of methods, which treat fluids neither at the molecular level nor as a continuous medium but as a medium consisting of particles with sizes larger than the sizes of individual molecules, occupies an intermediate place between molecular and Stokesian dynamics. In these methods, the motion of particles obeys the law of momentum conservation. This law is at the basis

of the Navier–Stokes equations. As a result, the hydrodynamically plausible motion of the fluid is provided without the direct solution of these equations. Of these methods, dissipative particle dynamics [108–112] and the lattice Boltzmann method [113–122] are most widely used. The advantage of these methods is that they are less time consuming than the molecular dynamics method (in some cases, than the Stokesian dynamics as well) and yet adequately reproduce hydrodynamic effects. It should be noted that these methods are based on continual equations of a continuous medium, fluid particles serving as discrete elements, due to which the equation in terms of partial derivatives can be reduced to the difference system of ordinary differential equations. These methods are essentially continual and their discreteness is purely computational. To the contrary, the molecular dynamics method is based on the equations of motion of particles/molecules (ordinary differential equations) determined by the balance between the quantity of motion and the interaction potential between particles, *i.e.*, it is the true discrete method.[6]

One of the modern approaches to simulation at the macrolevel, the so-called computational fluid dynamics (CFD), reproduces the behaviour of gas flows, Newtonian fluids and non-Newtonian fluids under different conditions. This extensively developed method was considered in numerous papers and monographs (see, for example, Refs 123–128), specialised journals and conferences. The detailed description of this method is beyond the scope of the present review. Let us only note that it is based on macroscopic equations (Navier–Stokes, *etc.*), whose solutions are sensitive to the boundary conditions. The available CFD program packages that implement numerical methods provide wide possibilities for solving problems of the dynamics of single-phase fluids, which are used in various fields of science and technology.[129] However, the application of these methods to simulation of suspensions presents difficulties because the boundaries move together with particles. These methods can be applied to systems composed of a small number of particles [130, 131] having simple and symmetrical geometry.[132, 133]

For this reason and also because the present review is devoted primarily to microrheological simulation, emphasis is given to methods oriented to simulation of suspension dynamics at micro- and mesoscopic levels. Let us briefly consider the mathematical backgrounds of some these methods.

a. Molecular dynamics method

The molecular dynamics method treats molecules and atoms as moving Newtonian particles. The equations of motion of classical mechanics for systems of interacting particles take the form

$$m_i \frac{\mathrm{d}^2}{\mathrm{d}t^2} x_i^{\langle\alpha\rangle} = -\frac{\partial}{\partial x_i^{\langle\alpha\rangle}} U\left(x_1^{\langle1\rangle}, \ldots, x_n^{\langle3\rangle}\right), \tag{57}$$

where $\alpha = 1-3$; $i = 1, 2, \ldots, n$, $x_i^{\langle\alpha\rangle}$ is the α-component of the vector x_i of the position of the ith particle from the set n, $U\left(x_1^{\langle1\rangle}, \ldots, x_n^{\langle3\rangle}\right)$ is the potential energy of the system, which is calculated by summing the energies of interparticle interactions, which depend on the distances between pairs of interacting particles

$$U\left(x_1^{\langle1\rangle}, \ldots, x_n^{\langle3\rangle}\right) = \frac{1}{2}\sum_{i\neq j} u\left(|x_i - x_j|\right).$$

An integration of the system of $3n$ equations of motion (57) with certain initial conditions gives the trajectories of particle motion. Particular (in the general case, arbitrary) coordinates and velocities of molecules are used as the initial conditions. In many cases, the velocities are chosen so that the total kinetic energy of the system corresponds to the given temperature. The density determined by the number of particles per unit volume can be used as another macroparameter. As a result of evolution, the system reaches an equilibrium state that depends on the temperature and the density, as well as on the interparticle interaction potential. The choice of the latter is of considerable importance because the properties of the system strongly depend on this parameter. On the one hand, the potential should correspond well to the physical meaning of the model and, on the one hand, it should be convenient for calculations. The surface effects at the boundaries of the system can, to a certain degree, be compensated with the use of the so-called periodic boundary conditions: if the particle moves outside the computational space through the right boundary, it simultaneously enters the space through its left boundary. As a result, the density and energy of the system are retained. To eliminate interactions of the particle 'with itself', the pair interaction potential is cut at a particular distance from the particle.

b. Stokesian dynamics method

The Stokesian dynamics method has been proposed for the first time by Brady and Bossis.[105] According to this method, the motion of n undeformable particles suspended in incompressible Newtonian fluid is described in a vector form by the equation

$$\boldsymbol{m}\frac{\mathrm{d}\boldsymbol{V}}{\mathrm{d}t} = \boldsymbol{F}^{\mathrm{h}} + \boldsymbol{F}^{\mathrm{c}}. \tag{58}$$

Here $\boldsymbol{m}$ is the generalised mass tensor (the moment of inertia tensor) of particles, $\boldsymbol{V}$ is the vector of dimensionality $6n$ of the translational and rotational velocities of particles, $\boldsymbol{F}$ are the vectors of forces acting on the particles (moments of force) of dimensionality $6n$: $\boldsymbol{F}^{\mathrm{h}}$ are the hydrodynamic dissipative forces caused by the motion of particles relative to the fluid and $\boldsymbol{F}^{\mathrm{c}}$ are the conservative forces, which can be dispersion interaction forces of colloidal particles or external forces (for example, the gravity force).

At low Reynolds numbers ($\mathrm{Re} \ll 1$), it is assumed that the hydrodynamic forces linearly depend on the velocities of particles

$$\boldsymbol{F}^{\mathrm{h}} = \boldsymbol{R}\boldsymbol{V}, \tag{59}$$

where $\boldsymbol{R}$ is the resistance tensor the elements of which characterise the influence of the medium on the particle.

In disperse systems consisting of particles with sizes of about 10^{-6} m (or smaller), the characteristic times of inertial displacements are very short. Hence, in some cases, the left-hand side of Eqn (58) can be ignored. Then the equation for the velocities of particles can be written as follows:

$$\boldsymbol{V} = -\boldsymbol{R}^{-1}\boldsymbol{F}^{\mathrm{c}}. \tag{60}$$

To calculate the velocities (and positions) of particles, a matrix inverse to $\boldsymbol{R}$ must be calculated in each step. Since the time consumed for the inversion of the resistance tensor increases proportionally to n^3, this operation is one of the main limitations in simulations of systems with a large number of hydrodynamically interacting particles. A simplified modification of the Stokesian dynamics can be used [107] to increase the efficiency of calculations. This method allows simulations of motion of highly concentrated suspensions in a shear flow. At high concentrations, the components in the resistance tensor responsible for long-range hydrodynamic interactions can be ignored due to a small gap between the particles. As a result, the matrix $\boldsymbol{R}$ becomes sparse and contains only components of short-range hydrodynamic interactions, which are calculated from the lubrication theory. This substantially simplifies the inversion of the matrix and results in proportionality between the calculation time and the square of the number of particles, due to which calculations of systems with much larger n become possible. To reveal the nearest neighbours of the particle, Voronoi and Delaunay tesselations were used.[107] In this approach, the space is partitioned into regions within which all points are closer to a particular point than to any of the other points (Fig. 12). This region is called the Voronoi region and it represents a convex polyhedron and a convex polygon in a three- and two-dimensional space, respectively. The Voronoi and Delaunay tesselations are widely used in simulations of ensembles of discrete particles arbitrarily arranged in the space. A detailed description of this geometric method was presented and the

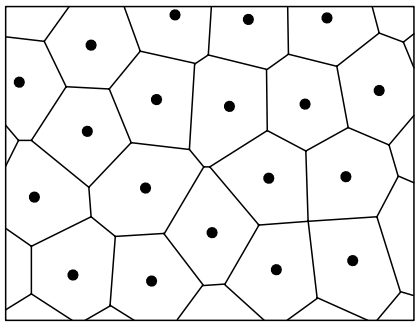


Figure 12. Voronoi tesselations of a point centre system in the plane.[134]

possibility of its application to the solution of particular physicochemical problems was considered in a monograph.[134]

In other modifications of the Stokesian dynamics, the Stokes law for an individual particle is used. It should be noted that this is valid only for low-concentrated suspensions.

The thermal motion of particles is described by the Brownian dynamics method. The stochastic force $\boldsymbol{F}^{\mathrm{B}}$ responsible for the Brownian motion is added to the right-hand side of Eqn (58). In this case, the equation for the velocity of particles (60) takes the form

$$\boldsymbol{V} = -\boldsymbol{R}^{-1}(\boldsymbol{F}^{\mathrm{c}} + \boldsymbol{F}^{\mathrm{B}}). \tag{61}$$

The force $\boldsymbol{F}^{\mathrm{B}}$ is chosen so as to fulfill the following conditions:

$$\langle \boldsymbol{F}^{\mathrm{B}} \rangle = 0, \tag{62}$$
$$\langle \boldsymbol{F}^{\mathrm{B}}(0)\boldsymbol{F}^{\mathrm{B}}(t) \rangle = 2k_{\mathrm{B}}T\delta(t)\boldsymbol{R},$$

where the angular brackets indicate the averaging over the total ensemble of particles and δ is the Dirac delta function.

The first condition means that the total result of the random Brownian forces is equal to zero. The second condition reflects the correlation between the random force at points of time 0 and t, which follows from the fluctuation-dissipative theorem of statistical physics. This condition is also indicative of the relationship between the Brownian and hydrodynamic forces, thus underlining their common nature.

The colloidal component of the force $\boldsymbol{F}^{\mathrm{c}}$ in Eqn (58) is a combination of the molecular attractive and electrostatic repulsive forces. At moderate concentrations of particles and at their moderate velocities, this component can be determined by summing the pair interaction potentials of particles based on the Deryaguin – Landau – Verwey – Overbeek (DLVO) theory.[36, 37]

c. Dissipative particle dynamics

The dissipative particle dynamics method has been proposed in the studies.[108, 109] As mentioned above, this method is based on the representation of a fluid as a combination of hypothetical particles at a supramolecular level (dissipative particles), the motion of which occurs according to the laws of classical mechanics under the action of conservative, dissipative and random forces [95]

$$\boldsymbol{F}_i = \sum_{j \neq i} \left[\boldsymbol{f}^{\mathrm{c}}(\boldsymbol{r}_{ij}) + \boldsymbol{f}^{\mathrm{d}}(\boldsymbol{r}_{ij}, \boldsymbol{V}_{ij}) + \boldsymbol{f}^{\mathrm{r}}(\mathbf{r}_{ij}) \right], \tag{63}$$

where $\boldsymbol{F}_i$ is the total force acting on the ith particle.

At first glance, this method is similar to the Brownian dynamics method. The radical difference is that Eqn (63) corresponds to forces acting on fluid particles rather than on dispersed particles.

The conservative force $\boldsymbol{f}_{ij}^{\mathrm{c}}$ can be obtained, for example, from the interaction potential between the particles i and j. The dissipative force $\boldsymbol{f}_{ij}^{\mathrm{d}}$ corresponds to the friction force that depends on the relative velocities of particles,

$$\boldsymbol{f}^{\mathrm{d}}(\boldsymbol{r}_{ij}, \boldsymbol{V}_{ij}) = -\gamma\omega^{\mathrm{d}}(r_{ij})(\boldsymbol{V}_{ij}\boldsymbol{e}_{ij})\boldsymbol{e}_{ij},$$

where $\boldsymbol{r}_{ij} = \boldsymbol{r}_i - \boldsymbol{r}_j$, $\boldsymbol{V}_{ij} = \boldsymbol{V}_i - \boldsymbol{V}_j$, γ is the coefficient that controls the friction force, the function $\omega^{\mathrm{d}}(r_{ij})$ describes the change in the friction coefficient with distance and $\boldsymbol{e}_{ij}$ is the unit direction vector $\boldsymbol{r}_{ij}$. The random force $\boldsymbol{f}_{ij}^{\mathrm{r}}$ is described by the equation

$$\boldsymbol{f}^{\mathrm{r}}(\boldsymbol{r}_{ij}) = \sigma\omega^{\mathrm{r}}(r_{ij})\xi_{ij}\boldsymbol{e}_{ij}.$$

Here σ determines a random pair interaction force, the function $\omega^{\mathrm{r}}(r_{ij})$ describes the change in the random force with distance, ξ_{ij} is a random value characterised by the normal distribution law and the unit variance, $\xi_{ij} = \xi_{ji}$.

The parameters γ and σ and the functions $\omega^{\mathrm{d}}(r_{ij})$ and $\omega^{\mathrm{r}}(r_{ij})$ are specified so as to fulfill the following conditions:[95]

$$\omega^{\mathrm{d}}(r_{ij}) = \left[\omega^{\mathrm{r}}(r_{ij})\right]^2,$$
$$\sigma^2 = 2k_{\mathrm{B}}T\gamma.$$

Dissipative particles that move under the acton of these forces interact with colloidal particles according to the mechanics laws thus providing their displacement and simulating the hydrodynamic and Brownian effects. Another essential difference between this method and the Brownian dynamics is that calculations according to the method under consideration ignore the momentum conservation in the system. In this case, the number of particles in the system is virtually the only unchangeable parameter. The equations of dissipative particle dynamics are written so as to provide the automatic fulfillment of the momentum conservation law, thus imparting the hydrodynamically realistic (satisfying the Navier – Stokes equation) behaviour to the system over rather wide time and space scales.

Consequently, the dissipative particle dynamics method makes it possible to go to the macroscopic level of pure fluids due to which certain properties of fluids (for example, the viscosity [110, 111]) can be calculated. Usually, dissipative particles are considered as spheres with fixed diameters and masses. However, Flekkoy and Coveney [112] suggested that the dissipative particle dynamics method be extended to the microscopic level by identifying dissipative particles with the Voronoi polyhedra of different sizes (Fig. 13). The Voronoi tesselation of dissipative particles based on the configuration of a system makes it possible to allocate computational burden depending on the required degree of detailing (a higher degree is required in narrow channels between colloidal particles than in the fluid bulk). This increases the flexibility and efficiency of the method and makes it possible to

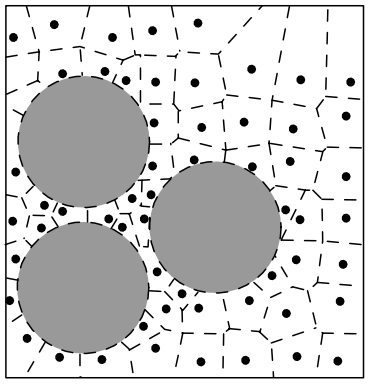


Figure 13. Scheme illustrating the applicability of the Voronoi tesselation in the dissipative particle dynamics method.[112]
Dissipative particles are identified with Voronoi regions. Four different length scales are presented: the scale of large colloidal particles, two scales of dissipative particles (between colloidal particles and in the fluid bulk) and the particle scale of the molecular dynamics method (solid points); the boundaries between dissipative particles are calculated depending on the arrangement of these scales.

apply this method to simulations of systems of concentrated suspensions, polymer solutions and flows in porous media with complex geometry on different length scales.

d. Lattice Boltzmann method

Among methods that are also based on the representation of fluids as discrete particles, the lattice Boltzmann method is worthy of note. In recent years, this method has been widely used for simulating hydrodynamic interactions in colloidal dispersions [113] and was described, for example, in the publications.[114–116] It belongs to the family of lattice methods and is based on the lattice gas model,[117] in which the space filled with a gas or fluid is divided into regions using a regular lattice. The motion of a fluid is described by the dynamics of hypothetical particles of unit mass, which are transferred, with certain probability, to the adjacent sites along the links of a fixed lattice (Fig. 14). In the sites, particle collisions take place. The collisions are considered taking into account the conservation laws. The time and space averages satisfy the Navier–Stokes equation. The advantage of the lattice gas method is its stochastic nature, which, however, is responsible for its main drawback, *viz*., a high noise level.

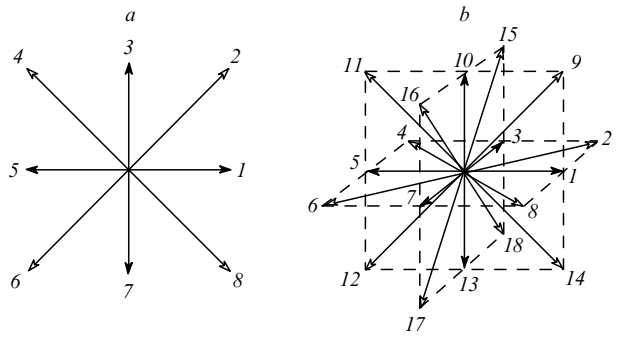


Figure 14. Possible displacements of a particle to the adjacent sites of two- (*a*) and three-dimensional (*b*) lattices.
(*1–18*) are the numbers of the positions. The diagonal directions are indicated by empty arrows. The vertical and horizontal directions are marked by solid arrows.

This method can be improved by using the Boltzmann equation for the description of lattice gases. In the relaxation time approximation, this equation takes the form

$$\frac{\partial}{\partial t} f(\boldsymbol{r},\upsilon,t) + \mathrm{v}\,\nabla f(\boldsymbol{r},\upsilon,t) = -\frac{1}{\tau}\left[f(\boldsymbol{r},\upsilon,t) - f^{\mathrm{eq}}(\boldsymbol{r},\upsilon,t)\right]. \qquad (64)$$

Here $f(\boldsymbol{r},\upsilon,t)$ is the Maxwell–Boltzmann distribution function, $f^{\mathrm{eq}}(\boldsymbol{r},\upsilon,t)$ is the equilibrium distribution function and τ is the relaxation time of the system due to particle collisions.

The Boltzmann equation can be transformed into the Navier–Stokes equations using the Chapman–Enskog expansion of Eqn (64). The Boltzmann equation for an incompressible Newtonian fluid can be solved in different ways with the use of lattice partitions. In the simplest modification of the lattice Boltzmann method, the summation in the lattice gas model is over particles, resulting in the replacement of this parameter with the density $f_i(\boldsymbol{r},t)$ of particles with velocities $\boldsymbol{c}_i$ in this region of the lattice. The velocities $\boldsymbol{c}_i$ are chosen so that a particle can either move to the adjacent lattice site during the time Δt or stay in its initial position. The mass and momentum conservation laws must be fulfilled. In this case, the main hydrodynamic parameters, by analogy with the parameters of the kinetic gas theory, are the moments of different orders of a random value $\boldsymbol{c}_i$. For example, the local fluid density is the zero-order moment

$$\rho(\boldsymbol{r},t) = \sum_i f_i(\boldsymbol{r},t);$$

the local momentum density is the first-order moment

$$\rho\boldsymbol{v} = \sum_i f_i(\boldsymbol{r},t)\boldsymbol{c}_i;$$

the momentum flux is the second-order moment

$$\Pi = \sum_i f_i(\boldsymbol{r},t)\boldsymbol{c}_i\boldsymbol{c}_i.$$

Calculations of the displacements of particles can be substantially simplified by linearising the collision operator (the function that relates the state of the lattice node before a collision to its state after the collision) in the deviation of the particle density from its equilibrium value. The best form of the operator for this type of collision was proposed by Bhatnagar, Gross and Krook (BGK) [118] and it provided the basis of the corresponding BGK models:[119]

$$f_i(\boldsymbol{r}+\boldsymbol{c}_i,t+1) = f_i(\boldsymbol{r},t) + \frac{1}{\tau}\left[f_i^{\mathrm{eq}}(\boldsymbol{r},t) - f_i(\boldsymbol{r},t)\right] + \boldsymbol{F}. \qquad (65)$$

Here $\boldsymbol{F}$ is an external force acting on a fluid (the mechanical force, the force of gravity, *etc*.). In Eqn (65), the unit time step was accepted, $\Delta t = 1$.

One of the possible ways of describing solid particles suspended in a fluid in terms of the lattice Boltzmann method is as follows.[120, 121] In a particle placed on a lattice, internal and boundary nodes are distinguished (Fig. 15). The node is considered as a boundary node if it shares at least on edge with nodes surrounding the fluid particle. For simplicity of calculations, it is sometimes assumed that the particle is filled with a hypothetical fluid. The collision operator is used for each node, including the boundary and internal nodes of the particle. The condition of the absence of sliding at the L/S interface in this method is generally fulfilled due to 'bounce-back' of fluid particles from the surface of colloidal particles with momentum conservation. The concept of the bounce-back of particles can be extended to the moving colloidal particles [120, 121]

$$f_i(\boldsymbol{r}+\boldsymbol{c}_i,t+1) = f_{i'}(\boldsymbol{r}+\boldsymbol{c}_i,t_+) + 2\rho_{\mathrm{f}}B_i(\upsilon_{\mathrm{w}}\boldsymbol{c}_i), \qquad (66)$$

where t_+ is the time immediately after a collision, i' is the lattice link, which is a direction of bounce-back, B_i are the coefficients that depend on the lattice partition, ρ_{f} is the fluid density, υ_{w} is the velocity of the wall (the surface of a colloidal particle) at a point $\boldsymbol{r}_{\mathrm{w}}$, and the latter term characterises the momentum transfer between the fluid and the solid wall.

The velocity υ_{w} is determined by the position of the centre of mass of the particle $\boldsymbol{r}_{\mathrm{c}}$ and its linear ($\boldsymbol{V}$) and angular ($\boldsymbol{\omega}$) velocities.

$$\upsilon_{\mathrm{w}} = \boldsymbol{V} + (\boldsymbol{r}_{\mathrm{w}} - \boldsymbol{r}_{\mathrm{c}}) \times \boldsymbol{\omega}.$$

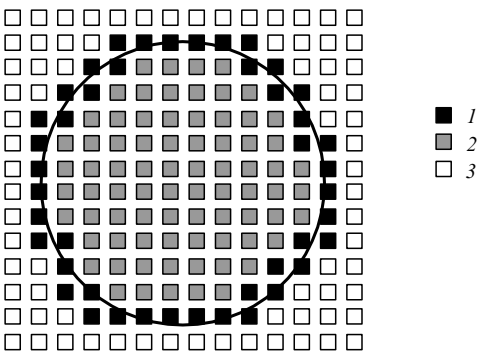


Figure 15. Schematic representation of a colloidal particle on a regular lattice.[135]
(*1–3*) are the boundary, internal and external (with respect to the particle) lattice nodes, respectively.

The overall hydrodynamic forces and moments of forces acting on a solid particle from the fluid can be determined by summation of the effects calculated according to Eqn (66) over all boundary nodes of a solid particle in each time step. The result is the movement of this particle under the action of the above-mentioned forces according to Newton's laws.

Since the density of particles, unlike their number, is not a discrete parameter, solutions obtained by the lattice Boltzmann method are not exposed to fluctuations associated with discreteness of the number of particles. This is often an advantage of the method. However, in simulations of the Brownian motion, it is necessary to specify statistical deviations from the calculated positions. This can be done by introducing an additional random force into Eqn (65).[122] On the whole, the lattice Boltzmann method provides a detailed description of the behaviour of a fluid and is efficient from a computational standpoint, due to which this can be successfully used in simulations of flows with complex geometry, *i.e.*, flows in porous materials, the dynamics of colloidal suspensions, *etc.*

In the next Section, we consider selected results of computer simulation of the dynamics of S/L disperse systems obtained with the use of the above-mentioned methods.

2. Results of computer simulation of dynamics of disperse systems

In Russia, computer simulation of the suspension dynamics has been performed for the first time in 1999.[136] Dispersions of spherical quartz particles in water consisting of 100, 400 and 900 particles were examined. Only pair interactions of particles were taken into account. The interaction potential curve was constructed based on the DLVO theory. The simulation was performed by a simplified method of the Stokesian dynamics based on the Stokes law for a single particle. Under shear conditions, the formation of a region with a low concentration of a dispersed phase was observed. This was attributed to the formation of layers oriented along the shear direction in a suspension flow. Earlier, this phenomenon has been observed and studied experimentally. In subsequent studies, computer simulations of disperse systems under dynamic conditions were carried out by the authors of the present paper using simplified Stokesian dynamics method.

The behaviour of dispersions in a shear flow was simulated by specifying a constant shear gradient at which the velocity of a fluid increases in the vertical direction. Particles in a fluid flow experience the Stokes force (viscous friction) exhibited by the fluid due to which they move together with the flow. The inertia component of the resistance force caused by the fluid was taken into account through the particle effective mass including, along with the particle mass, the added fluid mass, which is equal (in the case of spherical particles) to one-half of the mass of the displaced fluid,

$$m_{\mathrm{ef}} = m + \frac{\pi d^3 \rho_0}{12}.$$

The characteristics of the systems were as follows: $\eta_0 = 10^{-3}$ Pa s, $\rho_0 = 10^3$ kg m^{-3}, $\rho = 2.6 \times 10^3$ kg m^{-3}, $\varphi = 20\%$–40%, $d = 5$–100 μm. The particle interactions were calculated by specifying a potential curve with two energy minima corresponding to long- and short-range coagulation. Since the particle sizes of the systems under consideration differ by at most two times, the interaction energy was taken to be equal for each pair of particles regardless of their sizes.

In simulations of the influence of the physicochemical inhomogeneity of the particle surface (its lyophilic–lyophobic mosaicity) on the character of flow of a disperse system, it was assumed that the lyophilic and lyophobic regions are uniformly distributed over the particle surfaces. The probability of the formation of a contact in a lyophilic region, which is proportional to the fraction of the lyophilic particle surface γ, was determined using a random number generator. Each time, interactions between two particles were calculated assuming the parameters

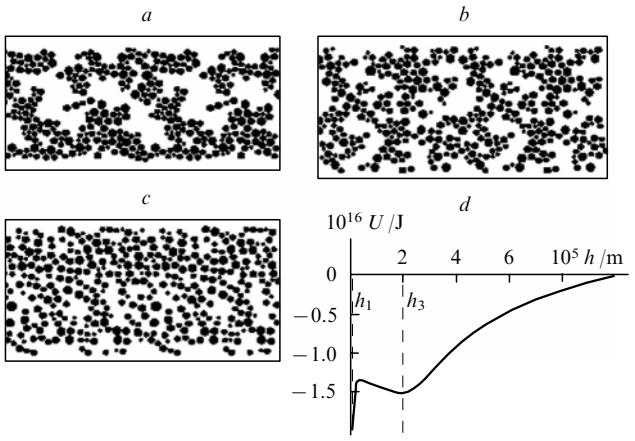


Figure 16. Flow of a disperse system with different degrees of lyophilicity (γ) of the particle surface (a–c) and the interaction curve of two lyophobic particles (d).
Parameters of the system: $n = 200$ particles; $\dot{\varepsilon} = 40$ s^{-1}, $\varphi = 40\%$; $d = 5$–10 μm; $\gamma = 0$ (a), 50 (b), 100% (c).

of the potential curve corresponding to a lyophilic or lyophobic contact. Since the presence of lyophilic regions results in weakening of attractions between particles, an increase in the degree of lyophilicity of the surface leads to an increase in the aggregation stability of the system (Fig. 16).

Computer simulations of disperse systems under dynamic conditions revealed many features of their behaviour characteristic of this state. The formation of layers and particle aggregates in flows of disperse systems was confirmed. Destruction and deaggregation of such systems can be performed by supplying additional energy as external mechanical forces (for example, vibration). Orthogonal oscillations of particles of disperse systems occur through vibrations of a dispersion medium in the direction perpendicular to the flow direction. This type of vibration effects causes a sharp increase in the fluidity of dispersions by promoting degradation of structured components in a disperse system, thus noticeably increasing its shear viscosity.[1–3]

All characteristic steps of formation of a layered structure in a dispersion flow are presented in Fig. 17. In the formation of layers oriented along the shear direction, long-range attractive forces that act on particles are of considerable importance. Numerical experiments showed that layered structures are not formed in systems consisting of particles with a weak force field effective at a

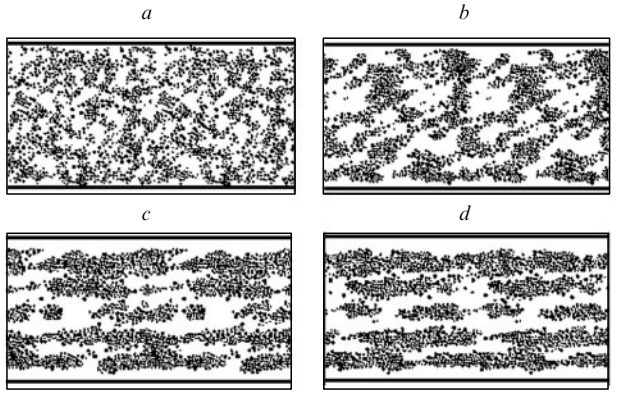


Figure 17. Sequence of the formation of a layered structure in a shear flow of a polydisperse system.
Parameters of the system: $n = 800$ particles; $\dot{\varepsilon} = 85$ s^{-1}, $\varphi = 35\%$; $d = 50$–100 μm; the time after the start of flow /s: (a) 0, (b) 0.05, (c) 0.3, (d) 0.5.

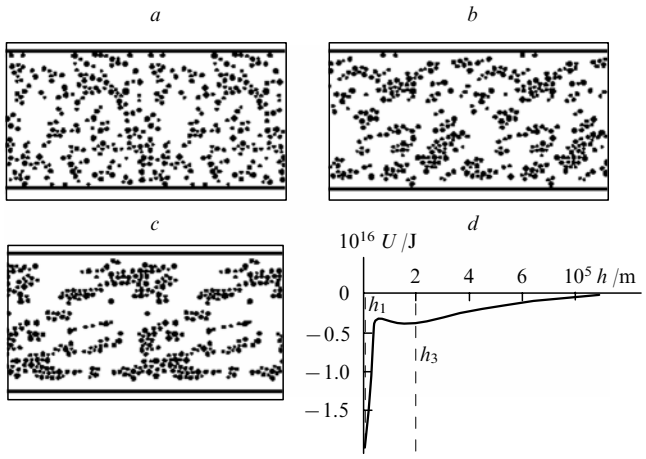


Figure 18. Illustration of the formation of aggregates in a dispersion flow due to dynamic coagulation of particles (*a*–*c*) and the interaction curve of two particles (*d*).
Parameters of the system: $n = 200$ particles; $\dot{\varepsilon} = 50\ s^{-1}$, $\varphi = 20\%$; $d = 50-100$ μm; the time after the start of flow /s: (*a*) 0, (*b*) 0.1, (*c*) 0.2.

short distance; instead, a nearly isotropic dynamic state is reached in a flow or (in the case of a deeper short-range potential well) aggregation occurs due to dynamic coagulation of particles (Fig. 18). The formation of a layered structure is responsible for anisotropy of the viscosity along and across the shear flow (in the latter case, the viscosity can be substantially higher).

Computer simulations of destruction under vibration were performed for a disperse system with particle sizes from 50 to 100 μm. Such large particles (which are nevertheless able to form coagulation structures due to cohesion [1, 39]) were chosen because of the necessity to develop inertial effects under vibration, which cause displacements of particles relative to each other and lead to destruction. The results of calculations of inertial dislpacements of particles relative to the medium depending on the particle size and the vibrational frequency are given in Table 1.[39] It can be seen that the larger the particle size and the higher the vibrational frequency, the larger the difference in the vibrational amplitudes of the particles and the medium. This means that destruction of systems formed by particles of colloidal sizes can occur only under ultrasonic vibrations.

Table 1. Relative inertial displacements of solid-phase particles in a liquid dispersion medium depending on harmonic vibrational frequency and the particle size.[39]

v /Hz	Relative displacement at particle radii /m				
	10^{-5}	5×10^{-5}	10^{-4}	5×10^{-4}	10^{-3}
50	0.9999	0.9611	0.7933	0.4977	0.4869
100	0.9995	0.9002	0.6760	0.4903	0.4853
200	0.9982	0.7953	0.5849	0.4869	0.4846
300	0.9963	0.7240	0.5501	0.4859	0.4843
400	0.9938	0.6760	0.5325	0.4853	0.4842
500	0.9910	0.6423	0.5219	0.4850	0.4841
1000	0.9723	0.5642	0.5016	0.4844	0.4840

The harmonic oscillations of the fluid along the *y* direction were specified according to the law

$$y_f = A \sin \omega t ,$$

where A is the vibrational amplitude, ω is the circular vibrational frequency and $\omega = 2\pi v$ (v is the frequency in Hz).

In vibrations, the vibrational amplitude of a dispersion medium was 0.1 mm and the frequency was 100–200 Hz. The choice of these parameters ensures a change in the ratio of the vibrational amplitudes of the particles and the medium for these vibrational frequencies in the ranges of approximately 1.0–0.7 and 0.9–0.5, respectively, thus providing conditions necessary for destruction.[83] However, the colloidal (surface) interaction forces of particles can be so large that the energy supplied by vibrations will be insufficient for destruction of structured ensembles in the dispersion.

As an example, the results of computer simulation of vibration effects on a disperse system under shear are presented in Fig. 19. It can be seen that the layered structure that is formed in a dispersion flow cannot be completely destroyed under vibrations of the medium. Moreover, in this case vibrations lead to coalescence of layers, *i.e.*, to the formation of larger structural inhomogeneities, which can apparently be accompanied by an increase in the shear viscosity of the disperse system. Presumably, this is one of the mechanisms of vibro-dilatancy, *viz.*, an increase in the dispersion viscosity under vibration.

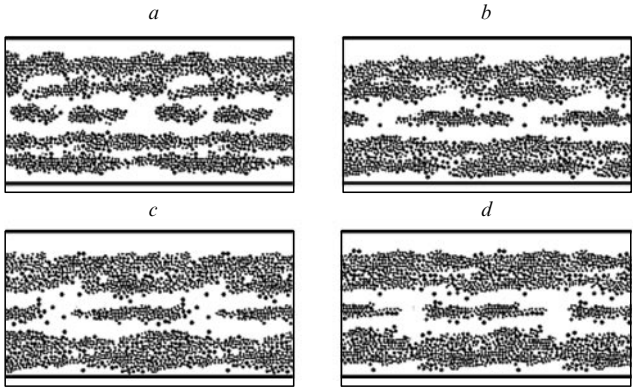


Figure 19. Changes in the layered structure under vibration.
Parameters of the system: $n = 800$ particles; $\dot{\varepsilon} = 85\ c^{-1}$, $\varphi = 35\%$; $d = 50-100$ μm; the time after the start of vibration /s: (*a*) 0,(*b*) 0.05, (*c*) 0.1, (*d*) 0.2.

Vibrations also cause 'grading' of particles according to sizes (see Fig. 19). This phenomenon is easy to explain as follows. Large particles are grouped predominantly with large particles; small particles, with small. This is due to the fact that particles are characterised by different vibrational amplitudes: small particles go ahead, whereas large particles go behind, resulting in the separation of the dispersion into fractions. At the same time, the possibility of adhering the smallest particles to the surface of large particles cannot be ruled out, which follows from the DLVO theory.[36, 37]

As mentioned above, the surface modification with surfactants facilitates destruction of coagulation structures because it eliminates the lyophilic–lyophobic mosaicity of the surface. As a result, virtually complete lyophilisation is achieved and, as a consequence, interactions between particles are weakened. In addition, coating of the surface with a surfactant layer creates a structural-mechanical barrier, which hinders dynamic coagulation.[1, 34]

Simulations of surfactant-modified systems were carried out under the assumption that neither surfactant desorption from the surface nor mechanochemical destruction of surfactants under dynamic forces take place. It was assumed that uniform coating of the particle surface is provided by surfactant molecules with short hydrocarbon radicals or with the use of a mixture of low- and high-molecular-weight surfactants.

The changes in the microstructure of surfactant-modified disperse systems in a shear flow can be seen from Fig. 20. The formation of a surfactant layer on the surface and its lyophilisation are accompanied by changes in the shape of the potential

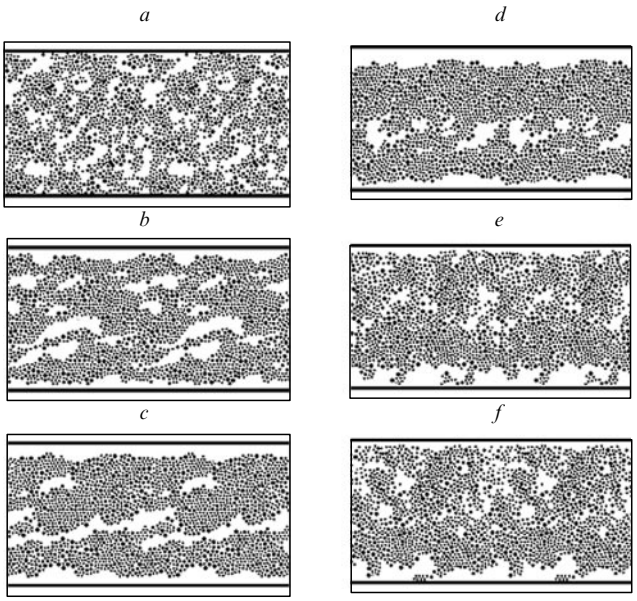


Figure 20. Formation ($a-c$) of an internal microstructure of a dispersion modified by treating the particle surface with surfactants and its destruction under vibration ($d-f$).
Parameters of the system: $n = 800$ particles; $\dot{\varepsilon} = 85\ s^{-1}$, $\varphi = 35\%$; $d = 50-100$ μm.

curve of particle interactions, for example, by a decrease in the depth of potential wells. Besides, the presence of a structural-mechanical barrier can prevent particles from approaching each other to a distance at which a short-range potential energy minimum exist. In this case, we can say that the short-range potential well is absent. Under these conditions, coagulation structures can be formed only due to long-range coagulation contacts, resulting in a lower density and a larger looseness of layers and other structured components in the dispersion (see Fig. 20). Under external vibrations, coagulation structures in such systems are rapidly destroyed (see Fig. 20 $d-f$) and a nearly isotropic dynamic state is achieved.

The data presented in Fig. 20 (and partially in Fig. 19) suggest also that discontinuities, which accompany the formation of a layered structure, are healed due to vibrations.[1,41]

The results of computer simulation of disperse systems under dynamic conditions confirm the above conclusion that surfactants combined with vibration create the desired synergetic effect. The use of the latter allows one to control the rheological properties of dispersions. This procedure can be used to perform isotropic destruction of coagulation systems accompanied by a decrease in the viscosity (an increase in the fluidity) of dispersions by several orders of magnitude.

Let us consider the results of computer simulation that demonstrate other possibilities of this method. Of a large number of publications on computer simulations of disperse systems, we discuss here studies most closely related to the problems under consideration.

The use of the full form of the Stokesian dynamics method in simulations of disperse systems provides a highly accurate description of the hydrodynamic effects, which however sharply increases the volume of calculations. In the studies,[101,106] the behaviour of a system consisting of 27 solid particles in a fluid was described by the Stokesian dynamics. The authors compared the results of these calculations with the data obtained by Brownian dynamics simulations, where the hydrodynamic effects are ignored, and demonstrated that it is important to take into consideration hydrodynamic interactions. In both cases, calculations were carried out for suspensions of solid spheres at a concentration $\varphi = 45\%$ in a simple shear flow. The plots of the equilibrium shear

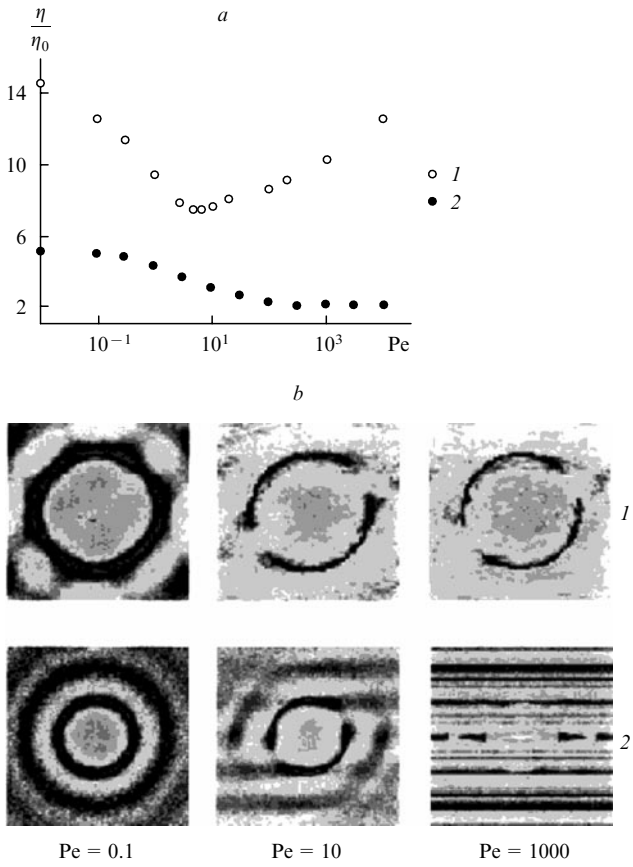


Figure 21. Computer simulation of changes in the viscosity (a) and the pair distribution function that characterises the microstructure of a suspension under shear (b).[101]
(1) Stokes dynamics, $n = 27$; (2) Brownian dynamics, $n = 1331$; $\varphi = 45\%$.

viscosity *vs*. the Peclet number are shown in Fig. 21 a. The viscosities were calculated by non-equilibrium statistical mechanics methods with the use of the Green–Kubo equation.[92,137] It can be seen from Fig. 21 that the quantitative contribution of hydrodynamic interactions consists of an increase in the suspension viscosity. However, the qualitative difference, *viz*., an increase in the viscosity at high shear rates (the dilatancy effect), is more important. The qualitative difference in the behaviour is associated with the shear-induced microstructure. The pair distribution functions of particles for three different shear rates (different Peclet numbers) are shown in Fig. 21 b. At small Peclet numbers, the microstructures formed in the presence of hydrodynamic interactions are similar to those formed in the absence of these interactions and are also similar to microstructures characteristic of fluids. Dark regions correspond to high probabilities of the presence of particles; light regions, to low probabilities. Rings corresponding to the nearest neighbours of the particle under consideration are clearly seen in the figure. The time necessary for calculations of a system consisting of 1331 Brownian particles is approximately equal to that necessary for calculations of a system consisting of 27 Stokesian particles. At Pe = 10, patterns that are calculated taking into account the hydrodynamics are also analogous to those, where the hydrodynamic effects are ignored, and demonstrate a shear-deformed microstructure.

The results obtained by the Stokesian and Brownian dynamics simulations, are qualitatively different at Pe = 1000. In the former case, a shear-deformed microstructure typical of fluids is seen but it is characterised by the more thinner nearest ring. In the studies,[101,138] the dilatancy effect was demonstrated to be directly related to this feature of the pair distribution function. In the absence of hydrodynamic interactions, the particles are arranged

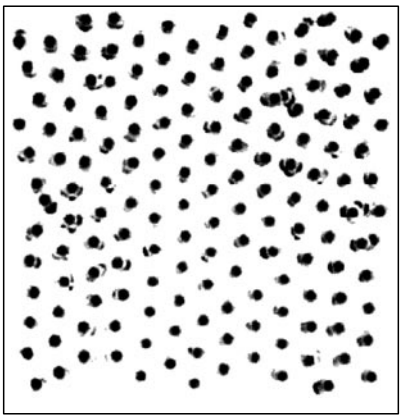


Figure 22. Brownian dynamics simulations of the arrangement of the particles in the plane perpendicular to the flow direction.[101]

in chains one after another, and the chains are located in hexagonal order in the plane perpendicular to the flow (Fig. 22). These chains are formed at high shear rates (when Brownian motion is of little importance): particles collide, rebound and adhere to other particles, again collide, rebound and so on until an ordered structure is formed. In the presence of hydrodynamic interactions, particles that are transferred by a flow do not rebound after collision and are held close to each other due to short-range hydrodynamic lubrication forces. Two particles rotating together in a flow hinder the formation of ordered chains. Therefore, the hydrodynamic effects influence both quantitatively and qualitatively the rheology and microstructure of colloidal dispersions. A detailed review of shear-induced microstructures in colloidal suspensions and analysis of the conditions of their formation and the role of hydrodynamic interactions between particles were given in the recent paper.[139]

It is particularly important to take into account the dilatancy effect under shear deformation and vibration accompanied by a spontaneous increase in the viscosity and shear stress because it inevitably influences the character of dispersion flows and the possibility of achieving the maximum fluidity.

In the study,[135] simulations of the dilatant properties of suspensions were carried out by the lattice Boltzmann method. The Couette flow of a suspension between two planar plates, which are located at a distance H from each other and move at a velocity u_w in opposite directions, was considered. The lattice partitions of dimensions 128×128 and 256×256 points were used. The particle diameter was 10 lattice nodes. The concentration of the solid phase was varied from 12% to 52%.

In the absence of the Brownian forces, the Reynolds number was used instead of the Peclet number for characterisation of shear flows

$$\mathrm{Re} = \frac{\rho_0 d^2 u_w}{\eta_0 H}\,.$$

The suspension viscosity was determined from the equation

$$\eta = \frac{\sigma_t}{\dot{\varepsilon}}\,,$$

where σ_t is the total shear stress on the walls and $\dot{\varepsilon} = 2u_w/H$ is the shear rate.

Plots of the relative suspension viscosity *vs.* the Reynolds number determined by computer simulations are given in Fig. 23 *a*. It can be seen that the higher is the suspension concentration, the earlier (*i.e.*, at lower shear rates) the dilatancy is observed. In the study,[135] these effects were related to the changes in the components of the total shear stress σ_f and σ_s corresponding to the liquid and solid phases. The changes in the relative contributions of σ_f/σ_t and σ_s/σ_t to the total shear stress depending on the Reynolds number at two suspension concentrations are

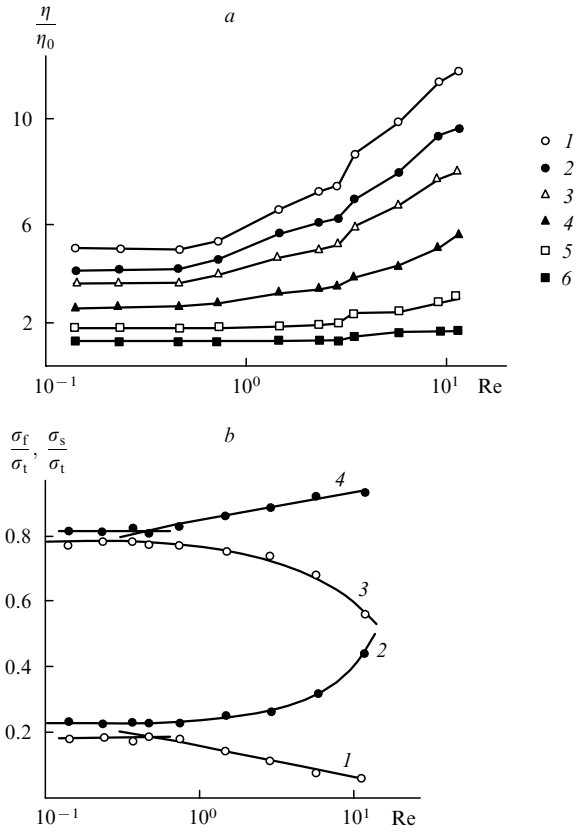


Figure 23. Suspension viscosity (*a*) and the shear stress corresponding to the fluid and solid phases (*b*) *vs.* the Reynolds number.[135]
(*a*): φ = 52 (*1*), 48 (*2*), 44 (*3*), 36 (*4*), 24 (*5*), 12% (*6*);
(*b*): σ_f/σ_t (*1*, *3*); σ_s/σ_t (*2*, *4*); φ = 12 (*2*, *3*) and 52% (*1*, *4*).

shown in Fig. 23 *b*. It can be seen that the components of the total shear stress are independent of the Reynolds number in the initial region and begin to change only at a particular value that depends on the concentration of the solid phase. This change consists of the increase in the contribution of the shear stress corresponding to solid-phase particles. A comparison of the curves presented in Fig. 23 *a*,*b* demonstrated that an increase in the suspension viscosity and an increase in the shear stresses in the solid phase are observed at the same Reynolds number, which is indicative of the relationship between these phenomena.

The shear stress corresponding to solid particles is an important parameter. Figure 24 shows the plot of the relative suspension viscosity *vs.* σ_s/σ_t. The points in the figure were determined for Re varying from 0.1 to 11.7. All calculated points corresponding to different Re and the concentrations of the solid phase fall in a single curve, *i.e.*, the suspension viscosity is a mere function of σ_s/σ_t and does not directly depends on either the concentration or the shear rate.

In the study,[135] the simple equation was derived for the dependence of the viscosity on the contribution of the solid phase to the total shear stress:

$$\frac{\eta}{\eta_0} = \frac{1}{1 - \sigma_s/\sigma_t}\,. \qquad (67)$$

However, the author of this work did not analysed the obtained results.

The results of computer simulations of the viscosity of a suspension consisting of solid spheres that were performed by different research groups using different methods [135, 140–145] agree well with the results of calculations according to the Krieger–Dougherty equation (4) and the experimental data (Fig. 25). This demonstrates the efficiency of computer simulations in studies of

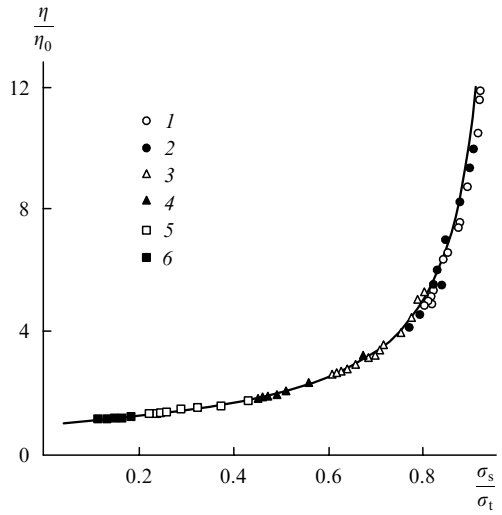


Figure 24. Relative suspension viscosity *vs*. the ratio σ_s/σ_t.[135] Points correspond to different concentrations and different Reynolds numbers. The solid line represents calculations according to Eqn (67). φ = 52 (*1*), 48 (*2*), 36 (*3*), 24 (*4*), 12 (*5*), 6% (*6*).

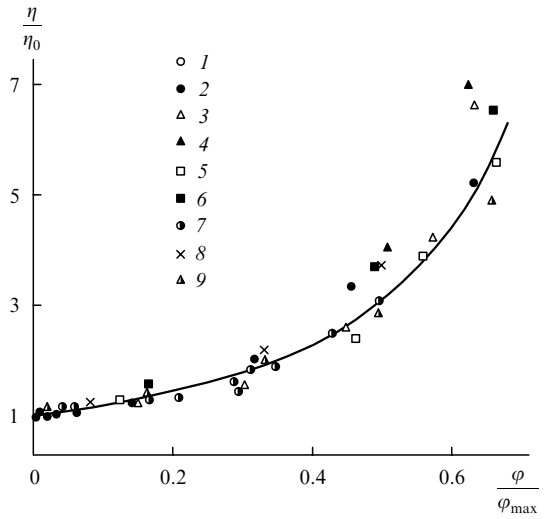


Figure 25. Theoretical data (curve) and data from computer simulations (points) of the suspension viscosity *vs*. the concentration. (*1*, *2*) Lattice Boltzman method (2D);[135,145] (*3*, *4*) Stokes dynamics (2D);[140,141] (*5*) lattice gas method;[144] (*6*) experiment;[30] (*7*, *8*) Stokes dynamics (3D);[142,143] (*9*) lattice Boltzman method (3D).[135]

the properties of disperse systems. The results of computer simulations were obtained at Re = 0.1 by the Stokesian dynamics,[140–143] the lattice gas method[144] and the lattice Boltzmann method[135,145] for two- (2D) and three-dimensional (3D) systems. The maximum particle concentrations were taken equal to 0.785 and 0.605 for 2D and 3D systems, respectively.

The results of computer simulation of a system of ellipsoidal particles by dissipative particle dynamics are presented in Fig. 26.[146] The particles with the aspect ratio $f = 5$ were considered. The suspension viscosity was calculated from the equation

$$\eta = -\frac{\sigma_{xy}}{\dot{\varepsilon}},$$

where σ_{xy} is the xy-component of the stress tensor, which is calculated in each time step. For dilute suspensions, the effective viscosity can be written as a first-order power series expansion in terms of the concentration of the solid phase φ

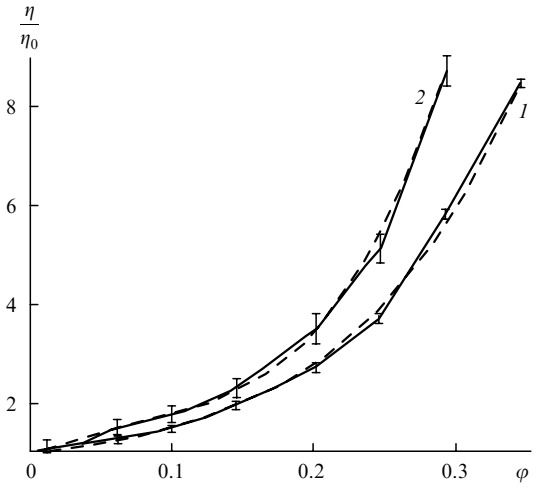


Figure 26. Relative viscosity of a suspension of ellipsoidal particles with the shape coefficient $f = 5$ *vs*. the concentration of the solid phase at dimensionless shear rates of 10^{-4} (*1*) and 10^{-5} (*2*).[146] Results of computer simulation were obtained by dissipative particle dynamics.

$$\frac{\eta}{\eta_0} = 1 + [\eta]\varphi.$$

According to the results of the investigation,[147] the degree of entanglement of rod-like particles increases with increasing concentration of a suspension, and the viscosity becomes proportional to the third power of the parameter φ. The results of simulations were approximated by third-order polynomials (see Fig. 26). The coefficient at the linear term $[\eta]$, which was obtained by approximation and interpreted as the 'intrinsic' viscosity of the system (5.67), is similar to the calculated value (5.78[146]) for ellipsoids with $f = 5$.

The results of computer simulations of disperse systems considered in the present review confirm many experimentally observed and theoretically substantiated data on the dynamic and rheological properties of dispersions. Analysis of these results shows the 'history' of the appearance and development of some phenomena and provides an insight into their mechanisms, which is not only of theoretical interest but also of practical importance because it offers additional possibilities for searching new ways of controlling the properties of disperse systems.

IV. Conclusion

The development of procedures for controlling the dynamic state of disperse systems is tightly associated with the development of theories and models that describe the behaviour of disperse systems under dynamic conditions. The main rheological theories of solid phase–liquid disperse systems in flows are reviewed. Emphasis is given to the problems associated with the description of the properties of aggregated and non-aggregated suspensions, because the degree and character of structure formation are responsible for the bulk rheological properties of disperse systems. The theoretical views on the causes and conditions of the appearance of discontinuities, *viz*., macroscopic inhomogeneities under structural deformation, are covered. The mechanism of the appearance of microinhomogeneities as discontinuities and the conditions of their healing were characterised for the first time by computer simulation methods. In a wide range of deformation rates, the evolution and elimination of inhomogeneities under vibrations are considered. The results of computer simulations of dynamics of disperse systems confirm many experimentally observed and theoretically substantiated features of the behaviour of disperse systems under dynamic conditions. Studies of these

features are of considerable importance not only because they provide the basis for the determination of the fundamental macroscopic and microrheological characteristics of these systems and elucidation of the relationship between these characteristics, but also because it is the controlled fluidity that is the most important factor for performing various heterogeneous chemical engineering processes (stirring, hydrotransport, catalysis, *etc*.).

Investigations of the dynamic state of disperse systems can help in revealing ways for providing dynamic aggregation stability and complete deaggregation of particles as the main condition for achieving the maximum fluidity of disperse systems with a decrease in the viscosity up to 8 – 11 orders of magnitude.

In studies of the ways and procedures for creating the maximum fluidity, it is necessary to use a combination of macro- and microrheological simulations taking into account intermolecular interactions, inertial and hydrodynamic effects under conditions of both continuous shear stress and a combination of this deformation with orthogonal oscillations and the addition of surfactants creating a structural-mechanical barrier on the particle surface. The parameters and conditions of the appearance of the latter require a theoretical description.

We thank E A Naumenko for help in performing computer simulations of disperse systems.

This review has been written with the financial support of the Russian Foundation for Basic Research (Project No. 03-03-32237).

References

1. N B Uriev *Usp. Khim.* **73** 39 (2004) [*Russ. Chem. Rev.* **73** 37 (2004)]
2. N B Uriev *Kolloidn. Zh.* **60** (5) 662 (1998) [a]
3. N B Uriev *Fiziko-khimicheskie Osnovy Tekhnologii Dispersnykh Sistem i Materialov* (Physicochemical Foundations of the Technology of Disperse Systems and Materials) (Moscow: Khimiya, 1988)
4. V V Krotov, A I Rusanov *Physicochemical Hydrodynamics of Capillary Systems* (London: Imperial College Press, 1999)
5. N B Uriev, A A Potanin *Tekuchest' Suspenzii i Poroshkov* (Fluidity of Suspensions and Powders) (Moscow: Khimiya, 1992)
6. A M Krivtsov, N V Krivtsova *Dal'nevostochnyi Matem. Zh.* **3** 254 (2002)
7. G K Batchelor, J T Green *J. Fluid Mech.* **56** 375 (1972)
8. C A Croxton, in *Liquid State Physics. A Statistical Mechanical Introduction* (Cambridge: Cambridge University Press, 1994) Ch. 2
9. W B Russel, F P Gast *J. Chem. Phys.* **84** 1815 (1986)
10. M Mooney *J. Colloid Interface Sci.* **6** 584 (1951)
11. T J Dougherty, Ph.D. Thesis, Case Institute of Technology, Cleveland, 1959
12. I M Krieger *Adv. Colloid Interface Sci.* **3** 111 (1972)
13. R Simha *J. Appl. Phys.* **23** 1020 (1952)
14. J Happel, H Brenner *Low Reynold Number Hydrodynamics* (2nd Ed.) (Leyden, The Netherlands: Noordhoff, 1973)
15. J Happel *J. Appl. Phys.* **28** 1288 (1957)
16. L D Landau, E M Lifshits *Teoreticheskaya Fizika. Gidrodinamika* (Theoretical Physics. Hydrodynamics) (Moscow: Fizmatlit, 2003) Vol. 6
17. N A Frankel, A Acrivos *Chem. Eng. Sci.* **22** 847 (1967)
18. M J Powell *Phys. Rev. B* **20** 4194 (1979)
19. G Marrucci, M M Denn *Rheol. Acta* **24** 320 (1985)
20. B H A Van der Brule, in *Proceedings of Xth International Congress on Rheology, Sydney, 1988* Vol. 2, p. 345
21. A A Potanin, N B Uriev, Ya Mevis, P Moldenaers *Kolloid. Zh.* **51** (3) 490 (1989) [a]
22. B S Endler *Inzh.-Fiz. Zh.* **37** 110 (1979) [b]
23. Yu Buyevich, I N Shchelchkova *Prog. Aerospace Sci.* **31** 121 (1978)
24. P D Patel, W B Russel *Colloids Surf. A* **31** 355 (1988)
25. J Mellema, M W M Willemse *Physica A* **122** 286 (1983)
26. A A Potanin, N B Uriev *J. Colloid Interface Sci.* **142** 385 (1991)
27. W J Frith Ph.D. Thesis, Katholieke Universiteit, Leuven 1986
28. I M Krieger, T J Dougherty *Trans. Soc. Rheol.* **3** 137 (1959)
29. C G de Kruif, E M F van Iersel, A Vrij, W B Russel *J. Chem. Phys.* **83** 4717 (1985)
30. J C Van der Werf, C G de Kruif *J. Rheol.* **33** 421 (1989)
31. J C Van der Werf, C G de Kruif, C Blom, J Mellema *Phys. Rev. A* **39** 795 (1989)
32. G K Batchelor *J. Fluid Mech.* **83** 97 (1977)
33. J O Hirschfelder, C F Curtiss, R B Bird *The Molecular Theory of Gases and Liquids* (New York: Wiley, 1966)
34. P A Rebinder *Izbrannye Trudy* (Selected Works) (Moscow: Nauka, 1979)
35. L A Abduragimova, P A Rebinder, N N Serb-Serbina *Kolloid. Zh.* **27** (3) 184 (1955) [a]
36. B V Derjaguin, N V Churaev, V M Muller *Poverkhnostnye Sily* (Surface Forces) (Moscow: Nauka, 1985)
37. E D Shchukin, A V Pertsov, E A Amelina *Kolloidnaya Khimiya* (Colloid Chemistry) (Moscow: Vysshaya Shkola, 2004)
38. N B Uriev, A A Potanin, Ya Mevis, P Moldenaers *Kolloid. Zh.* **51** (3) 535 (1989) [a]
39. N B Uriev *Vysokokontsentrirovannye Dispersnye Sistemy* (Highly Concentrated Disperse Systems) (Moscow: Khimiya, 1980)
40. N B Uriev, S I Choi *Kolloid. Zh.* **55** (3) 183 (1993) [a]
41. A A Potanin, N B Uriev *Kolloid. Zh.* **50** (3) 500 (1988) [a]
42. Y Baxter-Drayton, J F Brady *J. Rheol.* **40** 1027 (1996)
43. N V Churaev *Kolloid. Zh.* **50** (1) 108 (1988) [a]
44. A Ogawa, H Yamada, S Matsuda, K Okajima, M Doi *J. Rheol.* **41** 769 (1997)
45. D A R Jones, B Leary, D V Boger *J. Colloid Interface Sci.* **147** 479 (1991)
46. J W Goodwin, T Gregory, J A Stile *Adv. Colloid Interface Sci.* **17** 185 (1982)
47. L-B Chen, C F Zukoski *J. Chem. Soc., Faraday Trans.* **86** 2629 (1990)
48. T F Tadros *Adv. Colloid Interface Sci.* **68** 97 (1996)
49. R Hunter *Foundations of Colloid Science* (Oxford: Clarendon Press, 1992)
50. D Quemada *Eur. Phys. J.: Appl. Phys.* **1** 119 (1998)
51. D Quemada, C Berli *Adv. Colloid Interface Sci.* **98** 51 (2002)
52. V Trappe, D A Weitz *Phys. Rev. Lett.* **85** 449 (2000)
53. J Z K Zhou, T Fang, G Luo, P H T Uhlherr *Rheol. Acta* **34** 544 (1995)
54. D Quemada *Eur. Phys. J.: Appl. Phys.* **2** 175 (1998)
55. D Quemada *Eur. Phys. J.: Appl. Phys.* **3** 309 (1999)
56. P V Perepelkin, V M Starov, A N Fillipov *Kolloid. Zh.* **54** (2) 139 (1992) [a]
57. V G Zhdanov *Kolloid. Zh.* **60** (1) 5 (1998) [a]
58. D A Denny, R S Brodkey *J. Appl. Phys.* **33** 2269 (1962)
59. A M Stolin, S I Khudyaev, L M Buchatskii *Dokl. Akad. Nauk SSSR* **243** 430 (1978) [c]
60. B M Dolgonosov *Teor. Osnovy Khim. Tekhnol.* **35** 465 (2001) [d]
61. B M Dolgonosov *Teor. Osnovy Khim. Tekhnol.* **36** 592 (2002) [d]
62. J Cai, N Lu, C M Sorensen *J. Colloid Interface Sci.* **171** 470 (1995)
63. P Meakin, A T Skjeltorp *Adv. Phys.* **42** 1 (1993)
64. F E Torres, W B Russel, W R Schowalter *J. Colloid Interface Sci.* **145** 51 (1991)
65. M K Wu, S K Friedlander *J. Colloid Interface Sci.* **159** 246 (1993)
66. E J Windhab *Appl. Rheol.* **10** 134 (2000)
67. I Ya Ladyzhinskii, G N Urieva, Ya Mevis, N B Uriev *Kolloid. Zh.* **54** (1) 91 (1992) [a]
68. I Ya Ladyzhinskii, G N Urieva, Ya Mevis, N B Uriev *Kolloid. Zh.* **54** (1) 97 (1992) [a]
69. I Ya Ladyzhinskii *Kolloid. Zh.* **54** (4) 80 (1992) [a]
70. N B Uriev, I Ya Ladyzhinskii *Kolloid. Zh.* **54** (4) 87 (1992) [a]
71. I Ya Ladyzhinskii, N B Uriev *Kolloid. Zh.* **54** (4) 95 (1992) [a]
72. I Ya Ladyzhinskii, N B Uriev *Kolloid. Zh.* **54** (4) 102 (1992) [a]
73. N B Uriev, I Ya Ladyzhinsky *Colloids Surf. A* **108** 1 (1996)
74. I Ya Ladyzhinsky, N B Uriev *Colloids Surf. A* **108** 13 (1996)
75. F Family, P Meakin, J M Deutch *Phys. Rev. Lett.* **57** 727 (1986)

76. R Lullien, R Botel *Aggregation and Fractal Aggregates* (Singapore: World Scientific Publ. Comp., 1987)
77. S Havlin *Fractals in Physics* (Amsterdam: North-Holland, 1986)
78. B N Ouriev, N B Uriev *J. Meas. Sci. Technol.* **16** 1 (2005)
79. V E Chernomaz, N B Uriev *Kolloid. Zh.* **39** (6) 1211 (1977) [a]
80. L I Peregudova, N B Uriev *Kolloid. Zh.* **46** (6) 1166 (1984) [a]
81. A A Potanin, N B Uriev *Teor. Osnovy Khim. Tekhnol.* **22** (4) 528 (1988) [d]
82. L D Landau, E M Lifshits *Teoreticheskaya Fizika. Mekhanika* (Theoretical Physics. Mechanics) (Moscow: Fizmatlit, 2001) Vol. 1
83. N B Uriev, I V Kuchin, E A Naumenko *Inzh.-Fiz. Zh.* **78** (5) 164 (2005) [b]
84. V N Izmailova, P A Rebinder *Strukturoobrazovanie v Belkovykh Sistemakh* (Structure Formation in Protein Systems) (Moscow: Nauka, 1974)
85. A A Potanin, N B Uriev *Kolloid. Zh.* **50** (4) 712 (1988) [a]
86. A A Potanin, N B Uriev *Kolloid. Zh.* **50** (3) 493 (1988) [a]
87. D Raabe *Model. Simul. Mater. Sci. Eng.* **12** R13 (2004)
88. M P Allen, D J Tildesley *Computer Simulation of Liquids* (New York: Oxford University Press, 1990)
89. R W Hockney, J W Eastwood *Computer Simulation Using Particles* (New York: McGraw-Hill, 1981)
90. D C Rapaport *The Art of Molecular Dynamics Simulation* (Cambridge: Cambridge University Press, 1995)
91. J Goodfellow *Molecular Dynamics* (London: Macmillan Press, 1991)
92. C A Croxton, in *Liquid State Physics. A Statistical Mechanical Introduction* (Cambridge: Cambridge University Press, 1994) Ch. 5
93. Yu K Tovbin (Ed.) *Metod Molekulyarnoi Dinamiki v Fizicheskoi Khimii* (Method of Molecular Dynamics in Physical Chemistry) (Moscow: Nauka, 1996)
94. F J Vesely *Computational Physics. An Introduction* (New York: Plenum, 1994)
95. D Frenkel, B Smit *Understanding Molecular Simulation* (San Diego: Academic Press, 2002)
96. V M Zamalin, G E Normann, V S Filinov *Metod Monte-Karlo v Statisticheskoi Termodinamike* (The Monte-Carlo Method in Statistical Thermodynamics) (Moscow: Nauka, 1977)
97. H N V Temperley, J S Rowlinson, G S Rushbrooke (Eds) *Physics of Simple Liquids* (Amsterdam: North-Holland, 1968)
98. K Binder (Ed.) *Monte Carlo Methods in Statistical Physics* (Berlin: Springer, 1979)
99. K Binder *The Monte-Carlo Method in Condensed Matter Physics* (Berlin: Springer, 1992)
100. F Guarnieri *J. Math. Chem.* **18** 25 (1995)
101. J F Brady *Chem. Eng. Sci.* **56** 2921 (2001)
102. R M Mazo *Brownian Motion: Fluctuations, Dynamics and Applications* (Oxford: Oxford University Press, 2002)
103. E Wajnryb, P Szymczak, B Cichocki *Physica A* **335** 339 (2004)
104. J C Chen, A S Kim *Adv. Colloid Interface Sci.* **112** 159 (2004)
105. J F Brady, G Bossis *Ann. Rev. Fluid Mech.* **20** 111 (1988)
106. D R Foss, J F Brady *J. Fluid Mech.* **407** 167 (2000)
107. R C Ball, J R Melrose *Physica A* **247** 444 (1997)
108. E J Hoogerbrugge, J M V A Koelman *Europhys. Lett.* **19** 155 (1992)
109. J M V A Koelman, E J Hoogerbrugge *Europhys. Lett.* **21** 363 (1993)
110. P Espanol *Phys. Rev. E* **52** 1734 (1995)
111. C A Marsh, P V Coveney *J. Phys. A* **31** 6561 (1998)
112. E G Flekkoy, P V Coveney *Phys. Rev. Lett.* **83** 1175 (1999)
113. A Ladd, R Verberg *J. Stat. Phys.* **104** 1191 (2001)
114. S Succi *The Lattice Boltzmann Equation for Fluid Dynamics and Beyond* (Oxford: Clarendon Press, 2001)
115. R Benzi, S Succi, M Vergassola *Phys. Rep.* **222** 145 (1992)
116. S Chen, G D Doolen *Ann. Rev. Fluid Mech.* **30** 329 (1998)
117. U Frisch, B Hasslacher, Y Pomeau *Phys. Rev. Lett.* **56** 1505 (1986)
118. P L Bhatnagar, E P Gross, M Krook *Phys. Rev.* **94** 511 (1954)
119. Y-H Qian, D d'Humiéres, P Lallemand *Europhys. Lett.* **17** 479 (1992)
120. O Behrend, R Harris, P B Warren *Phys. Rev. E* **50** 4586 (1994)
121. A Ladd *J. Fluid Mech.* **271** 285 (1994)
122. A Ladd *Phys. Rev. Lett.* **70** 1339 (1993)
123. J D Anderson Jr. *Computational Fluid Dynamics* (London: McGraw-Hill, 1995)
124. P Roach *Computational Fluid Dynamics* (Albuquerque: Hermosa Publishing, 1972)
125. P Wesseling *Principles of Computational Fluid Dynamics* (Berlin: Springer, 2001)
126. J J Bloomer *Practical Fluid Mechanics for Engineering Applications* (New York: Marcel Dekker, 2000)
127. J H Ferziger, M Perid *Computational Methods for Fluid Dynamics* (Berlin: Springer, 1996)
128. C A J Fletcher *Computational Techniques for Fluid Dynamics* Vols 1, 2 (Berlin: Springer, 1988)
129. A Sangani, M Guobiao *Phys. Fluids* **6** 1653 (1994)
130. W R Bowen, A O Sharif *Nature (London)* **393** 663 (1998)
131. J J Gray, B Chiang, R T Bonnecaze *Nature (London)* **402** 750 (1999)
132. Y Huang, J Feng, D D Joseph *J. Fluid Mech.* **271** 1 (1994)
133. J Feng, D D Joseph *J. Fluid Mech.* **303** 83 (1995)
134. N N Medvedev *Metod Voronogo–Delone v Issledovanii Struktury Nekristallicheskikh Sistem* (The Voronoi–Delaunay Method in the Studies of the Structure of Non-crystalline Systems) (Novosibirsk: Siberian Branch of the Russian Academy of Sciences, 2000)
135. A Shakib-Manesh, Ph.D. Thesis, University of Jyvaskyla, Jyvaskyla, 2003
136. N B Uriev, A V Cheremisov, A Yu Tkachev *Kolloid. Zh.* **61** (3) 413 (1999) [a]
137. G Nagele, J Bergenholtz *J. Chem. Phys.* **108** 9893 (1998)
138. J F Brady, J F Morris *J. Fluid Mech.* **348** 103 (1997)
139. J Vermant, M J Solomon *J. Phys.: Condens. Matter* **17** R187 (2005)
140. C Chang, R L Powell *J. Fluid Mech.* **253** 1 (1993)
141. J F Brady, G Bossis *J. Fluid Mech.* **155** 105 (1985)
142. J X Zhu, D J Durian, J Müller, D A Weitz, D J Pine *Phys. Rev. Lett.* **68** 2559 (1992)
143. J F Brady *J. Chem. Phys.* **99** 567 (1993)
144. A J C Ladd, M E Colvin, D Frenkel *Phys. Rev. Lett.* **60** 975 (1988)
145. C K Aidun, Y Lu *J. Stat. Phys.* **81** 49 (1995)
146. E S Boek, P V Coveney, H N W Lekkerkerker *J. Phys.: Condens. Matter* **8** 9509 (1996)
147. M Doi, S F Edwards *The Theory of Polymer Dynamics* (Oxford: Oxford University Press, 1986)

[a] — *Colloid. J. (Engl. Transl.)*
[b] — *J. Eng. Phys. Thermophys. (Engl. Transl.)*
[c] — *Dokl. Chem. (Engl. Transl.)*
[d] — *Theor. Found. Chem. Eng. (Engl. Transl.)*